The role of cortistatin in neuroimmune dysregulation underlying ischemic stroke

Castillo-González J[1], Buscemi L[2,3], Vargas-Rodríguez P[1], Serrano-Martínez I[1], Forte-Lago I[1], Price M[2,3], Hernández-Cortés P[4], Hirt L[2,3*], González-Rey E[1*].

[1]Institute of Parasitology and Biomedicine (IPBLN-CSIC), Granada, Spain; [2]University of Lausanne, Lausanne, Switzerland; [3]Lausanne University Hospital, Lausanne, Switzerland; [4]Medicine School, University of Granada, Granada, Spain

*Correspondence: elena.g@csic.es; lorenz.hirt@chuv.ch; Tel.: +34-958-181670

Summary

Ischemic stroke is the result of a permanent or transient occlusion of a brain artery, leading to irreversible tissue injury and long-term sequelae. Despite ongoing improvements, therapeutic failure remains notorious, and stroke remains the second leading cause of death worldwide. Neuroinflammation, blood-brain barrier (BBB) breakdown, and immune deregulation are the major hallmarks of the pathogenesis and outcomes of brain ischemia. Understanding the interconnected and complex mechanisms and the endogenous mediators that globally modulate these responses is essential for developing successful therapeutic strategies. In this context, our study focuses on cortistatin, a neuropeptide widely distributed in the central nervous and immune systems. The anti-inflammatory, immunomodulatory, and neuroprotective properties of cortistatin make it an attractive novel therapeutic agent against ischemic stroke. To this aim, we evaluated the potential effect of cortistatin in the widely-known preclinical model of stroke MCAO (middle cerebral artery occlusion) in young (3 months old) and middle-aged (6 months old) wild-type mice. We observed that late treatment with cortistatin (24 h after stroke) improved neurological score, induced smaller lesions, reduced/modulated glial response, astrocytic scar formation and BBB recovery, and decreased peripheral immune activity. This beneficial effect of cortistatin suggests that multimodal-based therapies may represent a novel treatment for ischemic stroke, holding great promise compared to interventions targeting only a single aspect of stroke pathophysiology. Moreover, we found that the absence of cortistatin in young and middle-aged cortistatin-deficient animals increased susceptibility to stroke and worsened prognosis (*i.e.,* severe neurological score, altered microglial response, impaired astrocyte scar, disrupted BBB, dysregulated angiogenesis, and exacerbated immune infiltration and peripheral response). Interestingly, cortistatin treatment reversed stroke outcomes in animals lacking this neuropeptide, which highlights the key role of cortistatin in regulating the intricate interplay between the nervous and the immune systems, modulating dysregulated cellular and molecular responses from both systems that could impact brain homeostasis. Together, our findings underscore the relevance of identifying the endogenous and therapeutic role of neuro-immune mediators underlying ischemic stroke, and emphasize the critical need to consider multifactorial therapeutic approaches administered at later times and across different ages and phenotypes to extend the current therapeutic window for most patients who do not meet the clinical criteria.

INTRODUCTION

Ischemic stroke is the result of a permanent or transient occlusion of a brain artery. The sudden lack of cerebral blood flow in these areas followed by the subsequent reperfusion triggers a rapid and complex cascade of genomic, molecular, and cellular events that may evolve over hours to days and weeks after the onset [1]. These pathophysiology incidents are diverse and include energy failure, oxidative stress, loss of cell homeostasis, excitotoxicity, neuronal death, microglia reactivity, glial scar formation, blood-brain barrier (BBB) breakdown, and peripheral immune response [2]. Importantly, most of these events are intricately and subsequently connected, often unfolding in parallel or simultaneously within a short time frame.

Despite several efforts, stroke remains the second leading cause of death worldwide. So far, intravenous rtPA or endovascular thrombectomy are the only available treatments. However, the narrow therapeutic window and the great number of side effects limit the availability of both treatments [3]. Moreover, the intricate and still not fully understood pathophysiology of stroke complicates its management, as a plethora of simultaneous cellular and molecular mechanisms involving the brain, vascular system, and peripheral organs are underlying. Therefore, there is an urgent need to fully comprehend the neuro-immunological context and the involved factors at the different stages of the ischemic pathology to facilitate appropriate and successful therapeutic approaches.

Cortistatin is a cyclic neuropeptide widely distributed in the central nervous system (CNS) and the immune system [4,5]. Despite sharing considerable homology, functions, and receptors (Sst1-5) with somatostatin, cortistatin displays unique functions in the nervous system and peripheral tissues [6,7] by interacting with other receptors different from those of somatostatin, including the ghrelin receptor (Ghsr), the Mas gene-related receptor X-2 (MrgX2), and a yet unidentified cortistatin receptor. Notably, cortistatin displays potent anti-inflammatory properties, protecting against the development and progression of several inflammatory and autoimmune disorders (reviewed in [4]). Moreover, cortistatin treatment exerts immunomodulatory and neuroprotective effects in models of neuroinflammatory/neuroimmune disorders, such as multiple sclerosis [8], meningoencephalitis [9], excitotoxicity [10], neuropathic pain [11], or Parkinson's disease [12]. In these disorders, cortistatin consistently decreases inflammatory mediators, modulates glial cell function, and maintains tissue-surveillance activities. Moreover, cortistatin plays a key role in BBB, mediating anti-inflammatory endothelial functions and exerting BBB reparative properties through organizing tight-junction proteins and reducing immune exacerbated responses [13]. Importantly, the absence of cortistatin is associated with an exacerbated pro-inflammatory basal state in the CNS and periphery, coupled with decreased expression of neurotrophic factors [4,8].

Therefore, given the neuroprotective, anti-inflammatory, and immunomodulatory properties, and its ability to regulate BBB, we hypothesize that cortistatin may be a key endogenous factor in

the dynamics of ischemic stroke damage and recovery mechanisms. This positions cortistatin as a promising therapeutic agent, particularly in regulating glial responses, vascular and barrier changes, and peripheral immune activation.

MATERIALS AND METHODS

Peptides

Mouse CST-29 was acquired from Bachem. The lyophilized peptide was dissolved into distilled water (final concentration 10^{-4} M).

Animals

The procedures described in this study were approved by the Animal Care and Use Board and the Ethical Committee of the Spanish National Research Council (Animal Care Unit Committee IPBLN-CSIC # protocol CEEA OCT/2017.EGR), and they were conducted in accordance with the guidelines from Directive 2010/63/EU of the European Parliament for the protection of animals used for scientific purposes. Transgenic mice lacking the cortistatin gene (*Cort*$^{-/-}$) were a generous gift of Dr Luis de Lecea (Stanford University, United States) generated and maintained within a C57BL/6J background, following the methods previously described [6]. Animals were housed in groups of ten mice per cage in a regulated environment (22 ± 1ºC, 60-70 % relative humidity), and subjected to a 12 h light/dark cycle (lights on at 7:00 a.m.). Food and water were provided *ad libitum*.

Transient middle cerebral artery occlusion model

Young (12 weeks old) and middle-aged (6 months old) *Cort*$^{+/+}$ and *Cort*$^{-/-}$ mice were subjected to MCAO model [14]. Mice were anesthetized under isoflurane (1.5-2 % in 70 % N_2O / 30 % O_2) using a facemask. Mice were administered meloxicam (2 mg/kg, subcutaneously, Norbrook) for post-surgery analgesia. Body temperature was maintained constant throughout the surgery using a heating pad. The regional CBF (rCBF) was monitored by laser Doppler flowmetry (moorVMS-LDF1, Moor Instruments) fixing a probe on the skull over the core area supplied by the MCA (approximately 1 mm posterior and 6 mm lateral from the bregma). Transient focal ischemia was induced by introducing a silicon-coated filament (701756PK5Re, Doccol) through the left common carotid artery into the internal carotid artery until reaching and occluding the middle cerebral artery. The filament was placed here for 20/35 minutes for young and middle-aged mice respectively. After this time the filament was withdrawn to allow reperfusion. Surgery was considered successful when the flow dropped down to < 20 % of the baseline during the occlusion, and when it reached > 50 % of the baseline after reperfusion. Mice were housed in their cage until sacrifice, with *ad libitum* access to food and water. Each cage was equipped with water-softened chow and recovery gel.

Cortistatin (3.45 µg/mouse in PBS) was intraperitoneally administered 24 h after MCAO. Controls were injected with the same amount of saline solution. Neurological score, behavioural

tests, ischemic volume determination, morphometric characterization of glial populations, and inflammatory response, were determined 48 h after surgery.

Neurological score

The functional outcome of each mouse was assessed by a neurological score evaluation each 24 h after MCAO and before sacrifice. Severity was graded from 0 to 3 evaluating motor, sensory, reflex, and balance using a compendium of previously published scales [15,16].

Ischemic lesion volume determination

48 h after MCAO surgery, mice were sacrificed by an overdose of intraperitoneal injection of ketamine (100 mg/kg, Ritcher Pharma) and xylazine (10 mg/kg, Fatro Iberica) and intracardially perfused with 4 % PFA. Brains were dissected and fixed in 4 % PFA for 24 h at 4 ºC and cryoprotected in 30 % sucrose for 48 h at 4 ºC. Brains were then frozen in isopentane in dry ice at - 25 ºC and stored at - 80 ºC until use. Brains were cut into 20 µm coronal sections with a cryostat.

Cresyl violet-stained sections (gradual hydration in ethanol, stained with 1 mg/ml of CV-acetate in distilled water, gradually dehydrated in ethanol, and clear in xylene) [15] were imaged under a Leica DM2000 Transmit stereomicroscope at 2.5x magnification. The infarct volume was calculated by multiplying the sum of the infarcted areas on each section by the spacing distance using the ImageJ Fiji free software.

Immunofluorescence

For immunofluorescence labelling, 20 µm free-floating sections were washed with PBS and blocked and permeabilized with PBS 1x, 1 % BSA, 0.1 % Triton X-100, and 5 % goat serum for 60 min at RT. Then, sections were incubated with primary antibodies anti-MAP2 (1:1000, Sigma), anti-Iba1 (1:1000, Wako), anti-GFAP (1:5000, Dako), anti-CD31/PECAM-1 (1:300, BD), anti-ZO-1 (1:100, Fisher), or APC-labelled anti-CD45 (1:200, BD) in PBS 1x, 1 % BSA, 0.1 % Triton X-100, and 5 % goat-serum O/N at 4 ºC. Next, sections were washed with PBS and incubated with the corresponding secondary Alexa Fluor-conjugated antibodies (1:1000, Sigma) and DAPI in PBS 1x, 1 % BSA, 0.1 % Triton X-100, and 2 % goat-serum for 60 min. Sections were mounted with Mowiol. For IgG staining, the procedure remained the same, but no primary antibody was used. Instead, an Alexa Fluor 594-conjugated goat anti-mouse IgG antibody was directly used. Images were taken with a LEICA DMi8 S Platform Life-cell microscope at 20x and with a confocal Leica TCS SP8 STED microscope at 63x.

Morphometric characterization

To comprehensively describe the complex and diverse morphology of microglia, and astrocytes after a stroke, we employed different morphometric analyses. First, selected individual microglia images within the specific brain region (*i.e.,* periinfarct area for studying glial scar and microglia) were randomly selected. Great care was taken to ensure that there was no overlap between cells and that the entire nucleus and branches were included. In total, 15-30 cells from each mouse

(n = 15-30) from a total of 3-6 mice (N = 3-6) were analysed. Images were processed with ImageJ Fiji software following a systematic protocol adapted from others [12,17,18]. First, the image was transformed to 8-bit grayscale and pre-processed to reduce background noise and enhance contrast. Second, images were binarized by applying a pre-established threshold. Next, extraneous pixels that did not correspond to cells were eliminated with the tools *Remove outliers* and *Despeckle*. In cases where the original image contained a significant amount of background noise, careful manual editing was performed.

After processing the images, the Skeleton and Fractal Analysis plugins of ImageJ Fiji software [19] were employed using the following parameters. For Skeleton Analysis, the number of junctions and maximum branch length were evaluated. For Fractal Analysis, perimeter, area, circularity (*i.e.,* how closely the shape of an object resembles a circle), span ratio (*i.e.,* the ratio of the axes of the convex hull from major to minor), convex hull area (*i.e.,* the area containing the entire cell shape enclosed by the smallest convex polygon), fractal dimension (*i.e.,* index of complexity), and lacunarity (*i.e.,* heterogeneity) were evaluated. See the user manual for more details.

Determination of inflammatory factors

To determine inflammatory factors, blood was collected by cardiac puncture, allowed to clot for 2 h at RT, and then centrifuged at 2,000 rpm for 10 min. The concentration of inflammatory mediators from serum was determined by sandwich ELISA assay. Briefly, maxisorb plates (Millipore) were coated O/N at 4 ºC with the capture antibody anti-IL-6, anti-IL-12 (BD Pharmigen) or anti-MCP-1 (PeproTech). Next, plates were washed with PBS/0.05%-Tween20, blocked with PBS/10% FBS for 2 h, and incubated at 4 ºC O/N with the samples and recombinant standards. Biotinylated detection antibodies (Serotec) were added for 1 h at RT. After washing, plates were incubated with avidin-HRP (Sigma) (1:500 in blocking buffer) for 1 h and developed with ABTS substrate (Sigma). Absorbance was measured at 405 nm with a spectrophotometer (Molecular Devices) and concentrations were determined according to the standard curve generated at the same time.

Statistical analysis

Data are expressed as the mean ± SEM. All experiments were randomized and blinded for researchers. The number of independent animals is shown (N) as well as the number of sections, cells, or structures analysed in each case (n). Statistical analysis was conducted using these independent values. Statistical differences comparing two groups were performed by using the unpaired Student's t test (for parametric data, and normal distribution) or the non-parametric Mann-Whitney U-test. For three or more groups with normal distribution and parametric data, one-way ANOVA with appropriate *post-hoc* tests for multiple comparisons was utilized (with a small number of data Bonferroni *post-hoc* test was preferentially used *vs* Tukey *post-hoc* test). Non-parametric data from three or more groups was analysed by Kruskal-Wallis test and Dunn *post-hoc* test. When standard deviations were assumed to be different, Brown-Forsythe and Welch ANOVA test were

applied with Dunnett T3 *post-hoc* test. Spearman´s correlation non-parametric test was used for correlation studies. All analyses were performed using GraphPad Prism v8.3.0 software. We considered P-values < 0.05 (two-tailed) as significant.

RESULTS

Cortistatin reduces infarct volume size after stroke

To determine the potential therapeutic effect of cortistatin, we studied neurological score and neuronal lesions of young and middle-aged mice after administering cortistatin at 24 h (Figure 1a). First, neurological score was determined, which analyses motor, sensory, reflex, and balance functions on a scale from 0 to 3 (see Methods). As expected, a greater proportion of middle-aged animals exhibited a high score compared to their younger counterparts. While cortistatin treatment did not have a significant impact on the neurological score in mice of both age groups, there was a trend observed. 45% of middle-aged mice exhibited exacerbated deficits, which subsequently improved following cortistatin administration as only 12% of the treated mice displayed a high neurological score (over 1.5) (Figure 1b).

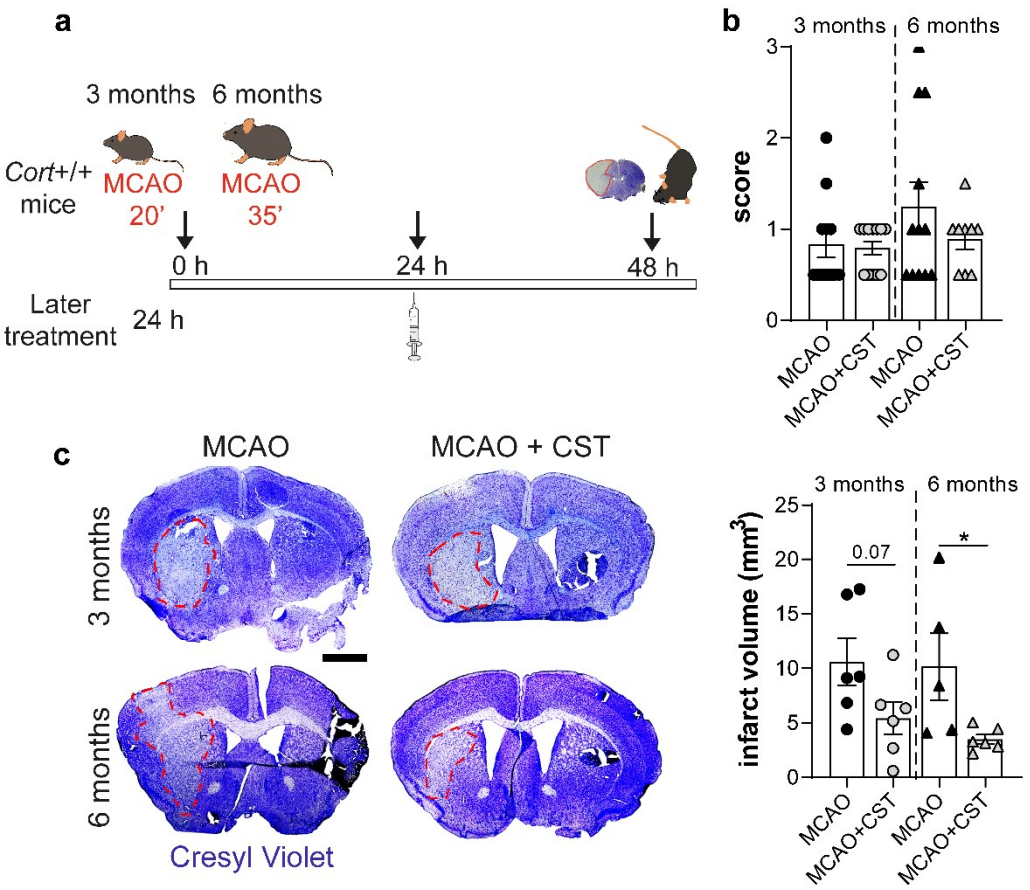

Figure 1. Cortistatin treatment reduces neuronal lesions in both young and middle-aged mice following acute stroke. a. Schematic representation of the timeline of the experiment. *Cort*$^{+/+}$ (wild-type) young (3 months old) and middle-aged (6 months old) mice subjected to MCAO and treated

with saline solution (MCAO) or with cortistatin (115 µg/kg) (MCAO+CST) at 24 h. At 48 h, score, and ischemic lesion determination were assessed. **a.** Neurological score was graded from 0 to 3 evaluating motor, sensory, reflex, and balance. **b.** Left, representative brain coronal sections stained with CV (Nissl bodies). Ischemic lesions are outlined with dashed red lines. Right, the ischemic volume across the brain was calculated by measuring ten CV-stained slices at 2 mm intervals in each mouse. Scale bar: 1,500 µm. Data are the mean ± SEM. N = 4-8 mice/group from 3 independent experiments. *$vs\ Cort^{+/+}$ MCAO, *$p \leq 0.05$.

Then, we determined neuronal lesion volumes using CV staining, a method that highlights intact neuronal cytoplasm in a robust purple colour, while dead neurons in the infarct area appear as faded light purple [20]. Importantly, we observed reduced infarct volumes in 3- and 6-month-old mice after cortistatin treatment particularly within the striatum (Figure 1c).

Cortistatin regulates microglial response in middle-aged mice suffering stroke

To further explore the role of cortistatin in stroke pathophysiology and neuronal injury, we investigated in more detail the local neuroinflammatory response in both young and middle-aged mice. First, microglia response was analysed (Figure 2a). Microglia exhibited increased proliferation in the ischemic core, feature that was augmented after cortistatin treatment in middle-aged mice (Figure 2b). Importantly, while microglia play a clearly defined role in the ischemic core (*i.e.,* phagocytosing dead neurons and secreting neurotrophic factors), microglia in the ischemic penumbra experiment intricate morphological and functional changes [21]. Since this area holds viable neurons, studying microglia dynamics within this area proves particularly compelling [21]. Given that the morphological alterations in microglia are closely linked to their reactivity states and serve as indicators of the severity of brain injury [17,22], we conducted Skeleton and Fractal Analysis (details found Methods) to analyse the microglia morphotype in the penumbra region in the mentioned mice.

As expected, both MCAO young and middle-aged animals showed a similar reactive microglial phenotype in comparison to their corresponding homeostatic contralateral microglia (Figure 2c). This reactive phenotype was marked by several characteristics, in one or both age groups, including a reduced number of junctions, branches with shorter lengths (Figure 2d), larger soma, and a smaller territory area (Figure 2e). Moreover, microglia from both age groups exhibited increased complexity (as reflected by fractal dimension) and span ratio, as well as reduced lacunarity and circularity (Figure 2f). In general, treatment with cortistatin appeared to modulate the reactivity of these cells, inducing a shift towards a more ramified microglia morphology (Figure 2c), similar to the homeostatic contralateral one, especially in middle-aged mice. However, the modulation differed between young and middle-aged mice. In middle-aged animals, microglia exhibited an enhanced number of junctions, longer branches (Figure 2d), larger territory area (Figure 2e), reduced complexity, decreased span ratio, and increased lacunarity and circularity, compared to MCAO mice (Figure 2f). Conversely, treatment with cortistatin in young mice preferentially impacted soma size (Figure 2e).

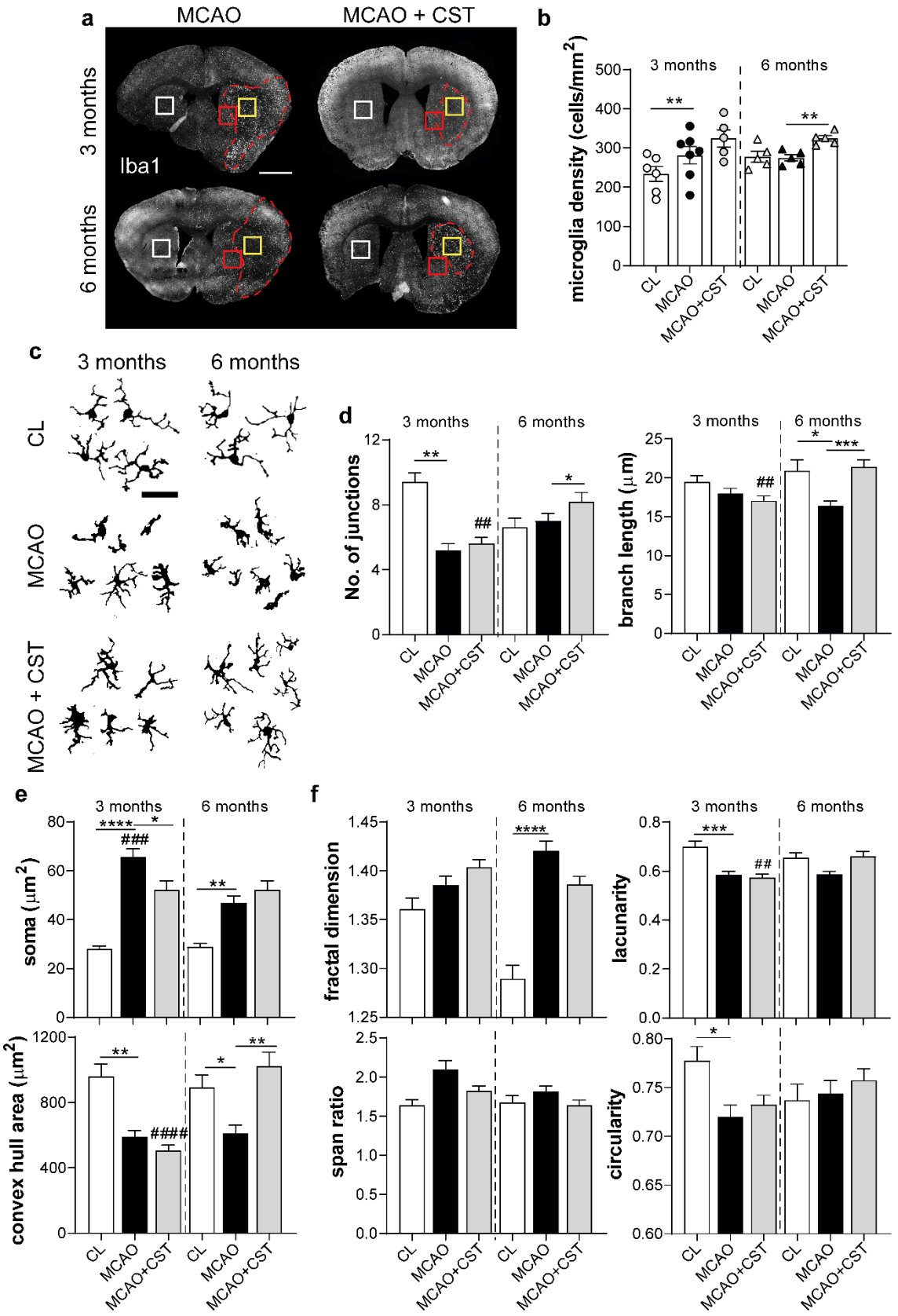

Figure 2. Cortistatin modulates microglia response. a. Representative brain coronal sections of *Cort*$^{+/+}$ young (3 months old) and middle-aged (6 months old) mice subjected to MCAO and treated with saline solution (MCAO) or with cortistatin (115 µg/kg) (MCAO+CST) at 24 h. Sections were stained with

Iba1 antibody to identify microglia. Dashed red lines represent ischemic core. Scale bar: 1,500 µm. **b.** Microglia density (number of cells/mm^2) was calculated in the ischemic core (striatum, yellow square) and the contralateral side (CL) (striatum, white square). **c.** Binary images of representative microglia were extracted from the ischemic penumbra (red square) and the CL (white square) from the different experimental groups. Scale bar: 30 µm. **d-f.** Morphological parameters evaluated in microglia. Skeleton Analysis was used to assess the number of junctions and their branch length (**d**). Soma size (**e,** top panel) was manually measured. Fractal Analysis was used to measure convex hull area (**e,** bottom panel), and fractal dimension/complexity, span ratio, lacunarity, and circularity (**f**). Data are the mean ± SEM. Analyses were conducted on 15-20 cells (n = 15-20) from at least three independent mice (N = 3). **vs Cort*$^{+/+}$ MCAO, $^{\#}$*vs* the same experimental group of 6-month-old mice. $^{*/\#}p \leq 0.05$, $^{**/\#\#}p \leq 0.01$, $^{***/\#\#\#}p \leq 0.001$, $^{****/\#\#\#\#}p \leq 0.0001$.

Cortistatin improved glial scar formation by promoting astrocyte reactivity

Given the observed impact of cortistatin on microglia reactivity, we extended our investigation to its modulation of the neuroinflammatory response of astrocytes (Figure 3a), as both cell types collaborate to limit the damage and prevent its spread [23]. We observed thicker glial scars in both age groups following cortistatin treatment, with a particularly pronounced effect in young animals (Figure 3a).

To further study the phenotype and function of these astrocytes in the formation of the glial scar, we also studied their morphology using Skeleton and Fractal Analysis. Importantly, we identified more reactive phenotypes in both age groups after cortistatin treatment (Figure 3c). These reactive astrocytes exhibited, in one or both age groups, fewer junctions, shorter branch lengths (Figure 3d), increased soma, and reduced convex hull area (Figure 3e). These changes were accompanied by a decreased complexity index (fractal dimension), greater span ratio, and reduced circularity and lacunarity (Figure 3f). This reactivity likely contributes to the development of thicker glial scars after cortistatin treatment and may be associated with the observed reduction in neuronal damage.

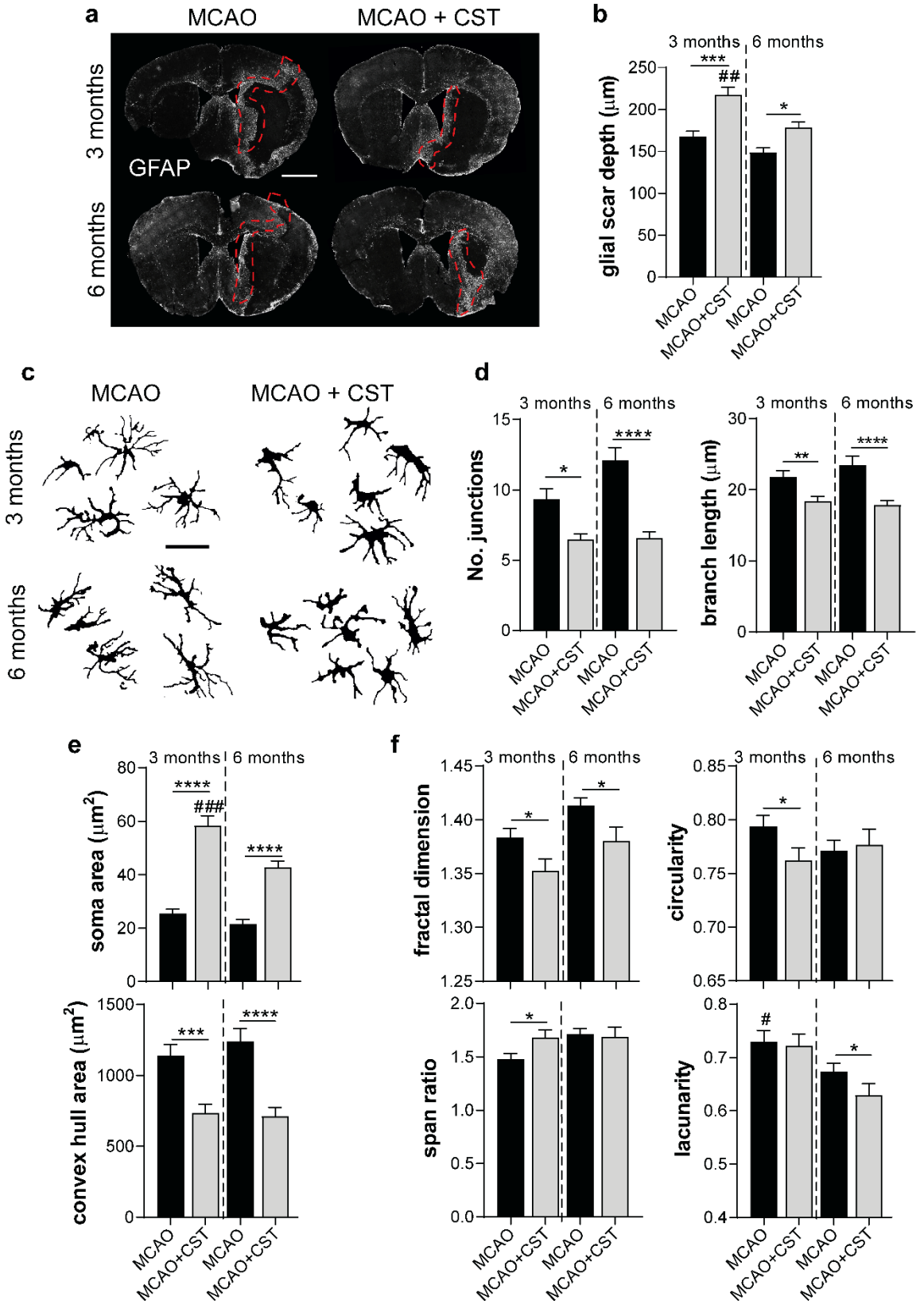

Figure 3. Cortistatin regulates glial scar formation and astrocytic functions. a. Representative brain coronal sections of *Cort*$^{+/+}$ young (3 months old) and middle-aged (6 months old) mice subjected to MCAO and treated with saline solution (MCAO) or with cortistatin (115 μg/kg) (MCAO+CST) at 24 h. Sections were stained with GFAP antibody to identify astrocytes. Scale bar: 1,500 μm. Dashed red lines represent astrocyte scar. **b.** Glial scar depth was measured along its extent in the different experimental

groups. **c.** Binary images of representative astrocytes from the glial scar were analysed. Scale bar: 30 µm. **d-f.** Morphological parameters were studied. Skeleton Analysis was used to assess the number of junctions and their branch length (**d**). Soma size (**e,** top panel) was manually measured. Fractal Analysis was used to measure convex hull area (**e,** bottom panel), and fractal dimension/complexity, span ratio, lacunarity, and circularity (**f**). Data are the mean ± SEM. Analyses were conducted on 15-20 cells (n = 15-20) from at least three independent mice (N = 3). **vs Cort*$^{+/+}$ MCAO, $^{\#}$*vs* the same experimental group of 6-month-old mice. $^{*/\#}p \leq 0.05$, $^{**/\#\#}p \leq 0.01$, $^{***/\#\#\#}p \leq 0.001$, $^{****/\#\#\#\#}p \leq 0.0001$.

These findings highlight the role of cortistatin as a crucial regulator of glial responses. In fact, treatment of both young and middle-aged animals 24 h after stroke does not deactivate glial cells but rather modulates their functional properties likely associated with protecting and rescuing from neurodegeneration.

Administration of cortistatin improves vascular dynamics after stroke regardless of age

One of the most prominent events in stroke is the breakdown of the BBB. It occurs shortly after the artery occlusion and can persist for several weeks after the onset of the stroke. Hypoxic conditions particularly affect brain endothelial cells (BECs), disrupting tight-junctions (TJs), leading to increased permeability and contributing to the development of vasogenic edema [24]. To comprehensively investigate the extent of BBB breakdown after stroke in these animals and whether cortistatin could modulate this important structure, we examined IgG leakage as a measurement of the cerebral extravasation of endogenous blood proteins. Importantly, IgG leakage was only observable in the infarct hemisphere, being reduced after cortistatin treatment in both age groups (Figure 4a), although these differences did not reach statistical significance (Figure 4b).

Among TJs, ZO-1 disruption has been widely reported after ischemia [25,26], being of pivotal importance in BBB dysfunction and subsequent recovery. To study how this TJ was affected during stroke development and after cortistatin treatment, we analysed ZO-1 disruption. Interestingly, ZO-1 in the ischemic core increased its expression after MCAO procedure compared to the contralateral side (Figure 4c), in both young and middle-aged mice (Figure 4d). However, ZO-1 presented a disorganized expression in both age groups after stroke, represented by an enhanced number of gaps. Although treatment with cortistatin revealed a similar presence of ZO-1 in the brain vessels, it significantly reduced the number of ZO-1 discontinuous expression in both age groups (Figure 4d).

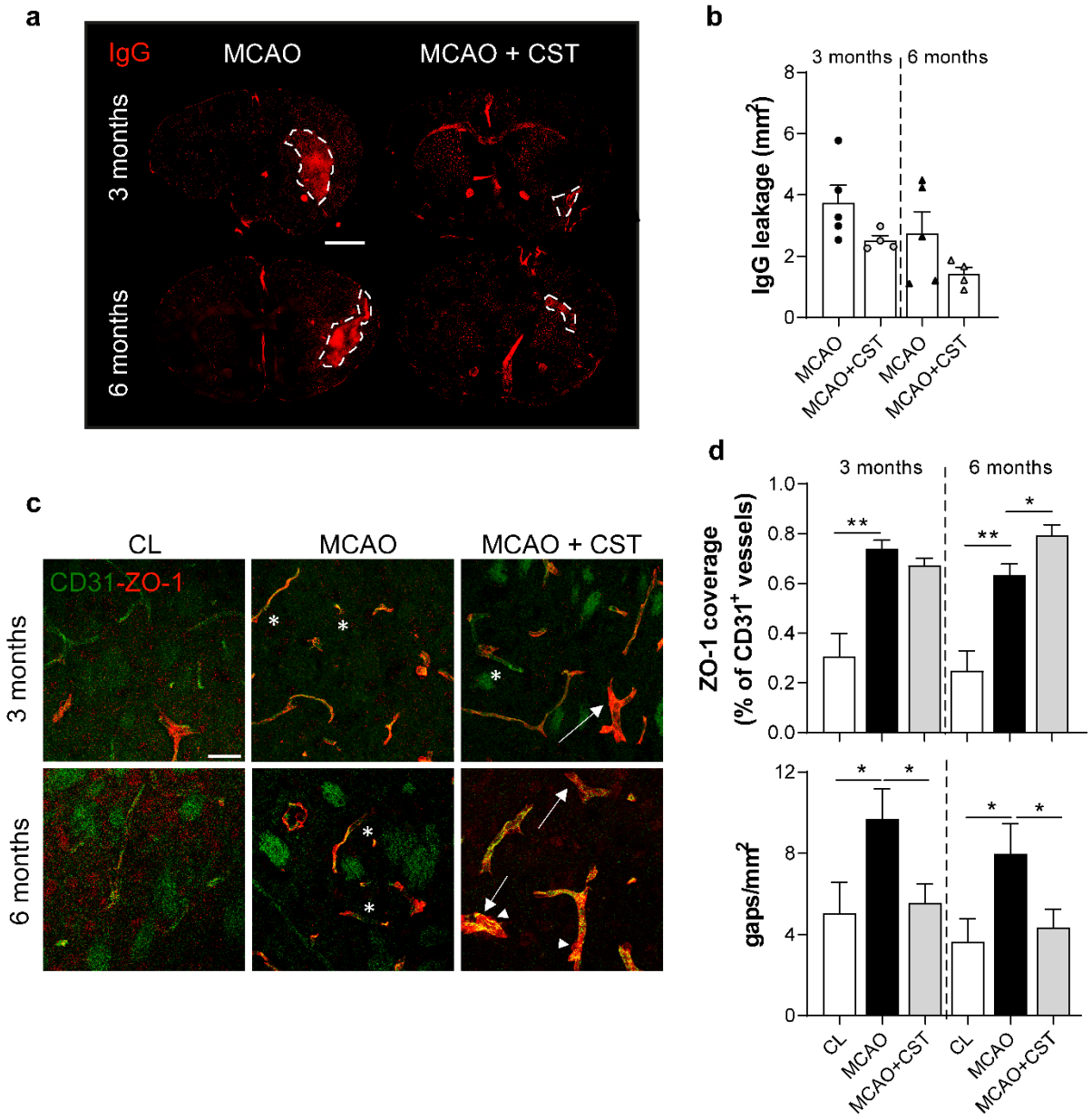

Figure 4. Cortistatin modulates BBB leakage and brain endothelium disruption. a. Sections of *Cort*$^{+/+}$ young (3 months old) and middle-aged (6 months old) mice subjected to MCAO and treated with saline solution (MCAO) or with cortistatin (115 µg/kg) (MCAO+CST) at 24 h, stained with a secondary antibody for IgG. IgG leakage is outlined with dashed white lines. **b.** IgG^{+} area was calculated as a measurement of IgG leakage from blood. Sections from 4-5 independent mice were analysed. Scale bar: 1,500 µm. **c.** Representative magnifications of the striatum of the different experimental groups following MCAO and their respective contralateral uninjured tissue (CL), stained with CD31 antibody for BECs (green) and ZO-1 (red) for TJs. ZO-1 gaps are highlighted with an asterisk and ZO-1 coverage recovery with arrows. Scale bar: 30 µm. **d.** ZO-1 coverage was measured as the % of positive ZO-1 area that was covering the vessel (CD31^{+} area) (top panel), as well as the number of gaps in ZO-1 structure (bottom panel). 3 different ROIs of 3-5 independent animals were analysed. Data are the mean ± SEM. **vs Cort*$^{+/+}$ MCAO. $^{*/}p \leq 0.05$, $^{**}p \leq 0.01$.

Of note, the dynamics of BBB disruption are complex, encompassing various stages of acute damage and subsequent regenerative responses, including angiogenesis and the modification of the vascular tree [27]. To investigate the importance of this process in reoxygenation and stroke

recovery, we examined the area occupied by vessels (CD31⁺) and their diameter in the striatum core and the contralateral side of the mentioned mice (Figure 5a). As anticipated, vascular density was enhanced in young and middle-aged mice after MCAO, significantly increasing after cortistatin treatment in young animals (Figure 5b). Although cortistatin did not influence vascular density in middle-aged animals, the treatment with the neuropeptide increased vessel diameter in both age groups (Figure 5c).

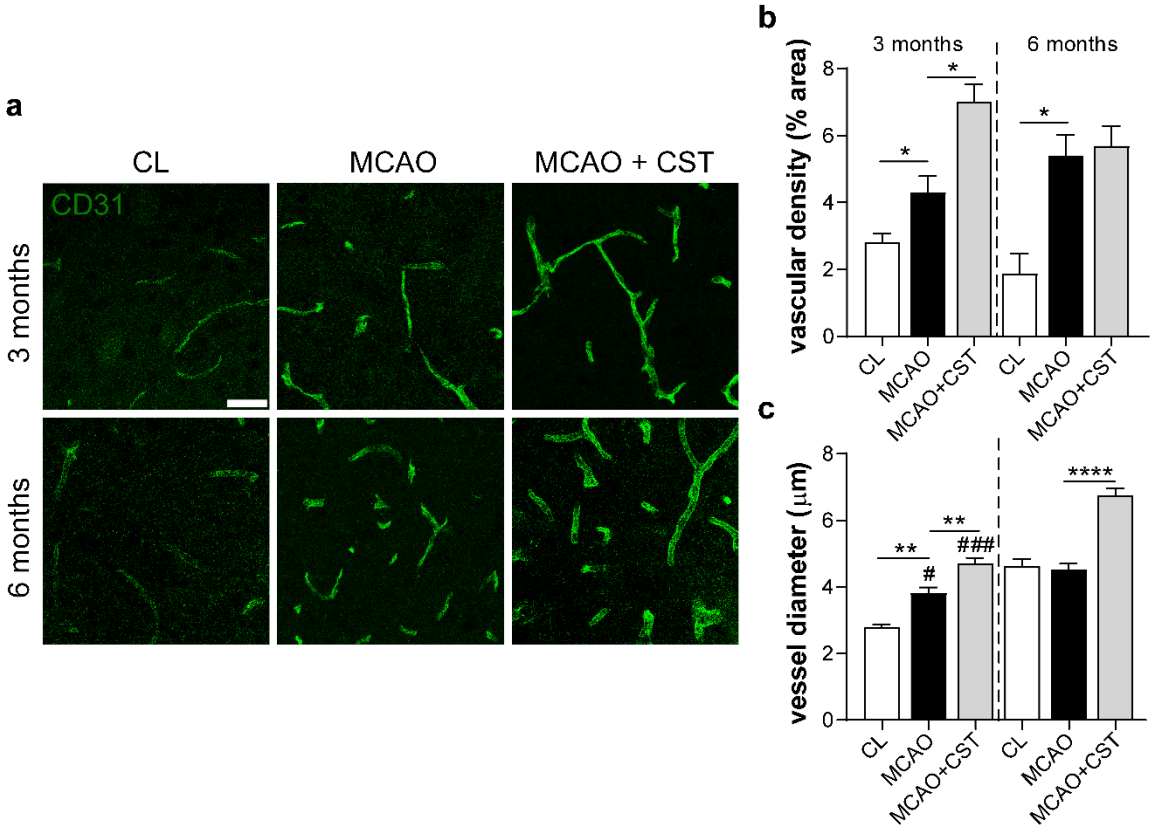

Figure 5. Cortistatin promotes angiogenesis and vascular remodelling after stroke. a. Representative images of BECs (CD31, green) from the striatum of *Cort*$^{+/+}$ young (3 months old) and middle-aged (6 months old) mice subjected to MCAO and treated with saline solution (MCAO) or with cortistatin (115 µg/kg) (MCAO+CST) at 24 h. Their respective contralateral uninjured tissue (CL) is also shown. Scale bar: 30 µm. **b.** Vascular density was measured as the area of positive CD31. **c.** Vessel diameter was measured manually. Data are the mean ± SEM. 3 different ROIs from 3-5 mice were analysed. For vessel diameter, 10-20 measures of each vessel from 5-10 vessels from each image were analysed. **vs Cort*$^{+/+}$ MCAO, *#vs* the same experimental group of 6-month-old mice. $^{*/\#}p \leq 0.05$, $^{**/\#\#}p \leq 0.01$, $^{***/\#\#\#}p \leq 0.001$, $^{****/\#\#\#\#}p \leq 0.0001$.

These results indicated that cortistatin protects against BBB permeability and brain endothelium disruption and promotes angiogenesis and vascular remodelling events, potentially resulting in greater reperfusion to the damaged area and facilitating recovery mechanisms.

Cortistatin reduces immune brain infiltration and attenuates ageing-exacerbated immune peripheral responses following a stroke

Following artery occlusion and prompted by ischemia and reperfusion, a coordinated inflammatory process unfolds, involving not only the brain but also peripheral organs [28]. As a result, there is a rapid adhesion of leukocytes and platelets to the endothelium that, facilitated by BBB breakdown, allows the infiltration of peripheral immune cells into the brain [29]. To study the role of cortistatin in the regulation of the peripheral immune response dynamics, we examined immune infiltration in the ischemic core of young and middle-aged mice using a general leukocyte marker (*i.e.,* CD45). Notably, $CD45^+$ cells were not detected on the contralateral side, whereas a significant number of cells infiltrated the ischemic region in MCAO mice regardless of age. Importantly, this immune infiltration significantly decreased after cortistatin treatment in both age groups (Figure 6a).

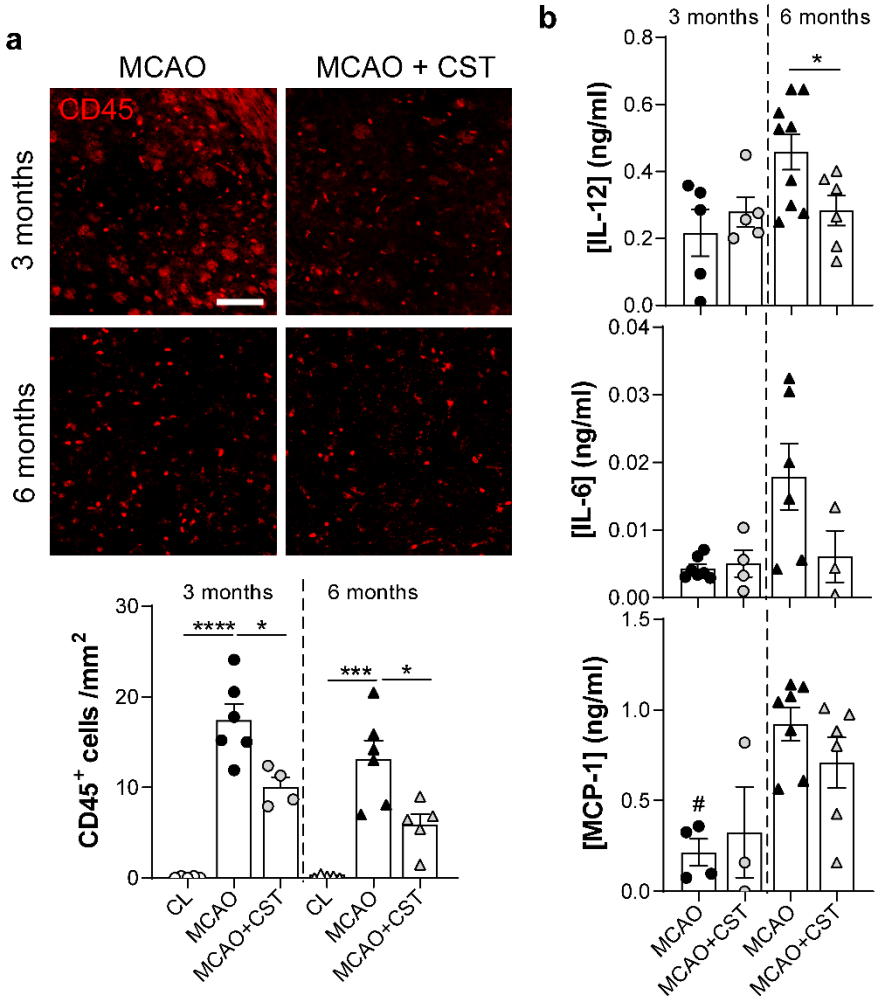

Figure 6. Cortistatin modulates immune infiltration and controls the peripheral immune response. a. Top panel**,** representative images from the striatum of *Cort*$^{+/+}$ young (3 months old) and middle-aged (6 months old) mice subjected to MCAO and treated with saline solution (MCAO) or with cortistatin (115 µg/kg) (MCAO+CST) at 24 h, stained with CD45 antibody (red) for leukocytes. Scale bar: 100 µm. Bottom panel, leukocyte density (number of cells/mm^2) was calculated in the striatum and in the contralateral side (CL) of the different experimental groups. **b.** IL-12, IL-6, and MCP-1

concentration (ng/ml) measured in serum by ELISA assay. N = 3-9 independent mice. Data are the mean ± SEM. *vs *Cort*$^{+/+}$ MCAO. *$p \leq 0.05$, ***$p \leq 0.001$, ****$p \leq 0.0001$.

After ischemia and BBB breakdown, cytokines and DAMPs generated by the brain injury enter the systemic circulation, reaching lymphoid organs and triggering the inflammatory response [28]. To characterize the impact of cortistatin on the systemic immune response 48 h after ischemia, we measured serum pro-inflammatory cytokines/chemokines including IL-12, IL-6, and MCP-1. Remarkably, these factors seemed to be enhanced in middle-aged animals when compared to young ones, although differences were not significant in any case. Treatment with cortistatin did not influence the levels of these mediators in young animals, but it showed a tendency to reduce the levels in middle-aged mice, particularly for IL-12 (Figure 6b).

To summarize, these results indicate that cortistatin treatment administered at later stages (24 h) reduces neuronal damage, potentially through the modulation of microglia reactivity and the formation of the astrocyte glial scar. Additionally, cortistatin regulates BBB dysfunction and facilitates recovery processes such as angiogenesis. Finally, cortistatin appears to regulate immune cell infiltration in the brain and partially modulates the peripheral immune response.

Deficiency of cortistatin exacerbates neurodegeneration, a condition that is reversed after treatment

Given the potential therapeutic effect of cortistatin, we next aimed to elucidate the endogenous role of this neuropeptide in stroke pathogenesis. Previous results from our group and others have described exacerbated inflammatory responses in cortistatin-deficient mice [8], worsened outcomes in models of inflammatory or neuronal damage [11,30,31], and the manifestation of a premature aging phenotype (preliminary data of the group). However, its role in stroke pathogenesis remains unknown. In light of this background, MCAO procedure was conducted in young (3 months old) and middle-aged (6 months old) cortistatin-deficient mice. Besides, *Cort*$^{-/-}$ mice were treated with saline solution or cortistatin at 24 h, to assess whether the treatment could impact the potential phenotype. Wild-type mice of the same age injected with saline were used as controls (the data were incorporated in the graphs as a reference). As described above, neurological score, behavioural performances, ischemic volume, glial population dynamics, BBB breakdown, and immune dynamics were analysed at 48 h (Figure 7a).

Young cortistatin-deficient mice displayed worsened neurological scores compared to wild-type mice (mean score 1-1.5, *i.e.,* moderate hypomobility, moderate motor incoordination, intermittent circling), which was significantly decreased by cortistatin treatment (Figure 7b). Similar trends were observed in middle-aged animals with 50% of *Cort*$^{-/-}$ mice exhibiting motor incoordination, intermittent circling, and tremor twitches (score 2-3). In contrast, although the differences were not significant, a reduced number of cortistatin-treated *Cort*$^{-/-}$ mice reached this high score (less than 24%) resembling to the clinical behaviour of MCAO *Cort*$^{+/+}$ mice (Figure 7b).

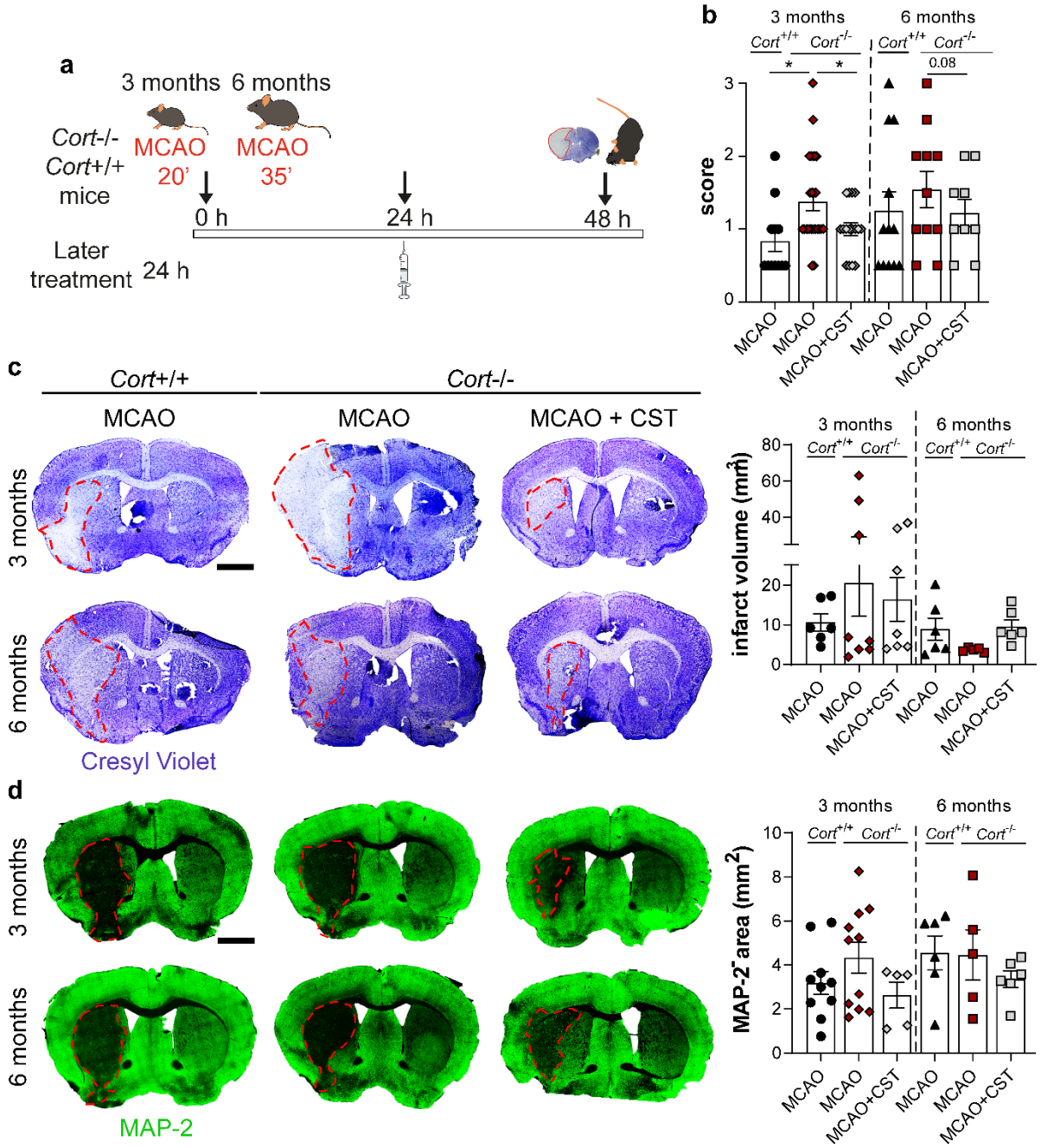

Figure 7. Cortistatin deficiency is associated with worse neurological deficits and neuronal lesions. a. Schematic representation of the timeline of the experiment. *Cort*$^{-/-}$ young (3 months old) and middle-aged (6 months old) mice subjected to MCAO treated with saline solution (MCAO) or with cortistatin (115 µg/kg) (MCAO+CST) at 24 h. Score at 48 h, neurological score and ischemic lesion determination were assessed. *Cort*$^{+/+}$ mice from each age group subjected to MCAO were used as controls. **b.** Neurological score was graded from 0 to 3 evaluating motor, sensory, reflex, and balance in the mentioned mice. **c.** Left panel, sections were stained with CV (Nissl bodies). Right panel, ischemic volume across the brain was calculated by measuring ten CV-stained slices at 2 mm intervals in each mouse. **d.** Left panel, MAP-2 immunostaining identified dendrites and axonal processes. Right panel, ischemic area was assessed by measuring MAP-2^{-} area in a representative selected coronal section. Data are the mean ± SEM. N = 6-12 mice/group from 3 independent experiments. **vs Cort*$^{-/-}$ MCAO *$p \leq 0.05$, *$p \leq 0.01$.

We then sought to investigate the ischemic lesion volume through evaluation of CV and MAP-2 in these mice. According to CV staining, young animals lacking cortistatin showed severe ischemic damage (over 30 mm^3) when compared to *Cort*$^{+/+}$ animals (Figure 7c). Surprisingly, we did not observe larger lesions in older *Cort*$^{-/-}$ mice by using CV (Figure 7c). However, when we analysed damage in the striatum using MAP-2 staining, we observed a trend towards larger lesions in *Cort*$^{-/-}$ mice at both ages (Figure 7d). Cortistatin treatment reverses the ischemic lesion in both age groups of the deficient mice to the MCAO wild-type lesions, hence reducing the exacerbated damage of both neuronal soma and dendrites, although the differences were not significant (Figure 7d).

In the absence of cortistatin, glial cells exhibited an impaired neuroinflammatory response which is modulated after cortistatin treatment

Given the exacerbated inflammatory responses in cortistatin-deficient mice [8], we proceed to investigate the neuroinflammatory response in these animals. Regarding microglia dynamics (Figure 8a), we observed an increase in microglia density in the infarct core of *Cort*$^{-/-}$ mice compared to their contralateral side in both age groups (Figure 8b). Besides, a higher number of cells were found in cortistatin-deficient mice after MCAO compared to 6-month-old wild-type animals. Although cortistatin treatment did not affect microglia density (Figure 8b), we noted a different reactive morphotype of these cells in young and middle-aged mice compared to their contralateral homeostatic counterparts and their corresponding wild-type mice (Figure 8c). In young MCAO mice deficient in cortistatin, we quantified a reduced number of junctions and branch length (Figure 8d), increased soma, reduced territory area (Figure 8e), increased fractal dimension and span ratio, and reduced lacunarity (Figure 8f). On the contrary, *Cort*$^{-/-}$ middle-aged mice showed a distinct morphotype pattern. In this case, hyper-ramification was significantly observed with a reduced number of junctions but larger branch lengths (Figure 8d), augmented soma (Figure 8e) but a greater occupied territory, and reduced fractal dimension and circularity (Figure 8f).

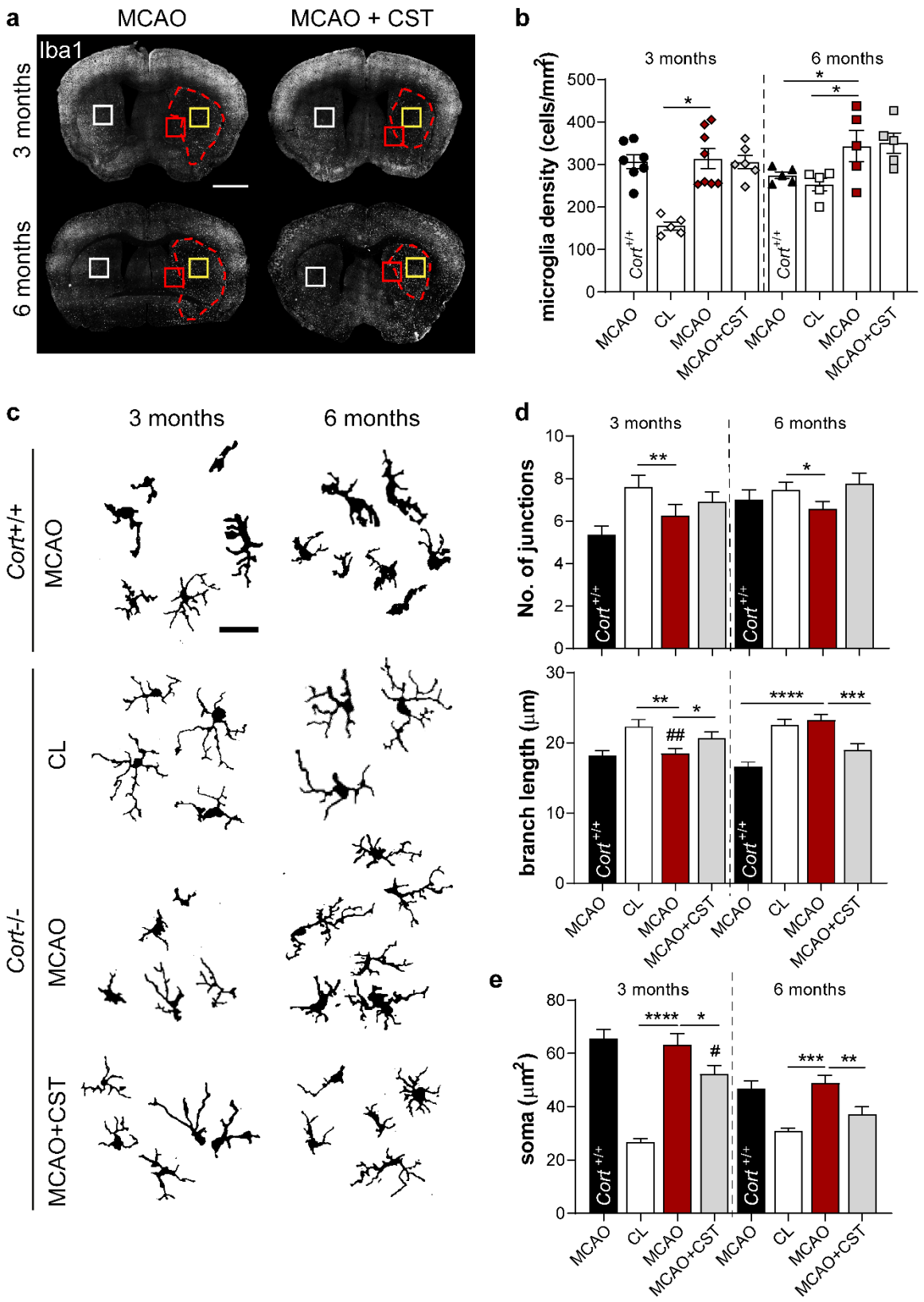

Figure 8. Part 1

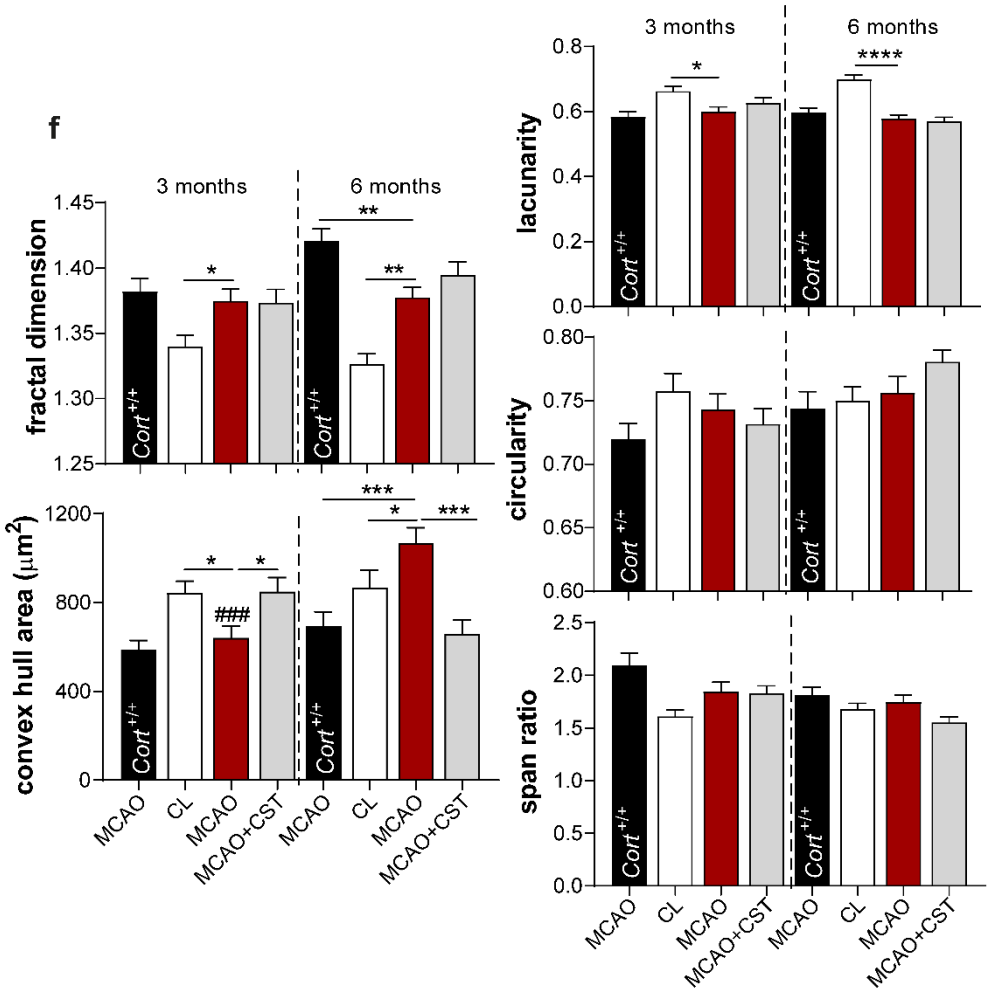

Figure 8. Part 2

Figure 8. The deficiency of cortistatin leads to microglia dysfunctional response, reversed by cortistatin treatment. Part 1 (a-e): a. Representative brain coronal sections of *Cort*$^{-/-}$ young (3 months old) and middle-aged (6 months old) mice subjected to MCAO and treated with saline solution (MCAO) or with cortistatin (115 µg/kg) (MCAO+CST) at 24 h, stained with Iba1 antibody to identify microglia. *Cort*$^{+/+}$ mice from each age group subjected to MCAO were used as controls. Dashed red lines outline the ischemic core. Scale bar: 1,500 µm. **b.** Microglia density (number of cells/mm^2) was calculated in the ischemic core (striatum, yellow square) and the contralateral side (CL) (striatum, white square) of the different experimental groups. **c.** Binary images of representative microglia were extracted from the ischemic penumbra (red square) and the CL (white square) from the different experimental groups. **d-f.** Morphological parameters evaluated in microglia. Skeleton Analysis (**d**) was used to assess the number of junctions (top panel) and their branch length (bottom panel). Soma size (**e**) was manually measured. **Part 2 (f):** Fractal Analysis was used to measure fractal dimension/complexity (top left) convex hull area (bottom left), lacunarity (top right), circularity (middle right), and span ratio (bottom right). Data are the mean ± SEM. Analyses were conducted on 15-20 cells (n = 15-20) from at least three independent mice (N = 3). **vs Cort*$^{-/-}$ MCAO, $^{\#}$*vs* the same experimental group of 6-month-old mice. $^{*/\#}p \leq 0.05$, $^{**/\#\#}p \leq 0.01$, $^{***/\#\#\#}p \leq 0.001$, $^{****/\#\#\#\#}p \leq 0.0001$.

Importantly, cortistatin modulated this phenotype in both age groups, leading to a mixed microglia population. While most features were partially reversed by cortistatin treatment, resembling microglia in MCAO wild-type mice, some properties such as soma size and complexity

mirrored microglia found in healthy wild-type animals (Figure 2). This suggests that in cortistatin-deficient animals, cortistatin may modulate microglia activation in a different way compared to wild-type mice, effectively reversing its dysfunctional phenotype.

Complementary, we studied astrocytic dynamics (Figure 9a). Surprisingly, an impaired glial scar was observed in cortistatin-deficient mice compared to wild-type controls, especially in the older ones, likely associated with age-related susceptibility (Figure 9b). The treatment with cortistatin reversed this feature up to baseline levels found in MCAO wild-type mice (Figure 9b). Considering this striking difference, we conducted a more detailed study of astrocyte morphology (Figure 9c). Notably, we observed that after MCAO astrocytes from both age groups lacking cortistatin displayed an unusual phenotype characterized by smaller non-ramified elongated forms. In more detail, they displayed fewer junctions, shorter branch lengths (Figure 9d), smaller soma, reduced territory coverage (Figure 9e), decreased complexity, increased span ratios, and reduced circularity and lacunarity compared to wild-type astrocytes following MCAO. However, most of these aberrant parameters were reversed by the neuropeptide treatment (Figure 9d-f), as astrocytes were switched into a more activated and presumably functional phenotype (Figure 9c).

In summary, these findings reveal that cortistatin deficiency is associated with a dysfunctional glial phenotype, likely contributing to the observed more severe neuronal damage. However, cortistatin treatment reverses this dysfunctional phenotype and appears to shift microglia and astrocytes phenotype to a more reactive state. This change is likely essential in these animals to restrict neuronal damage.

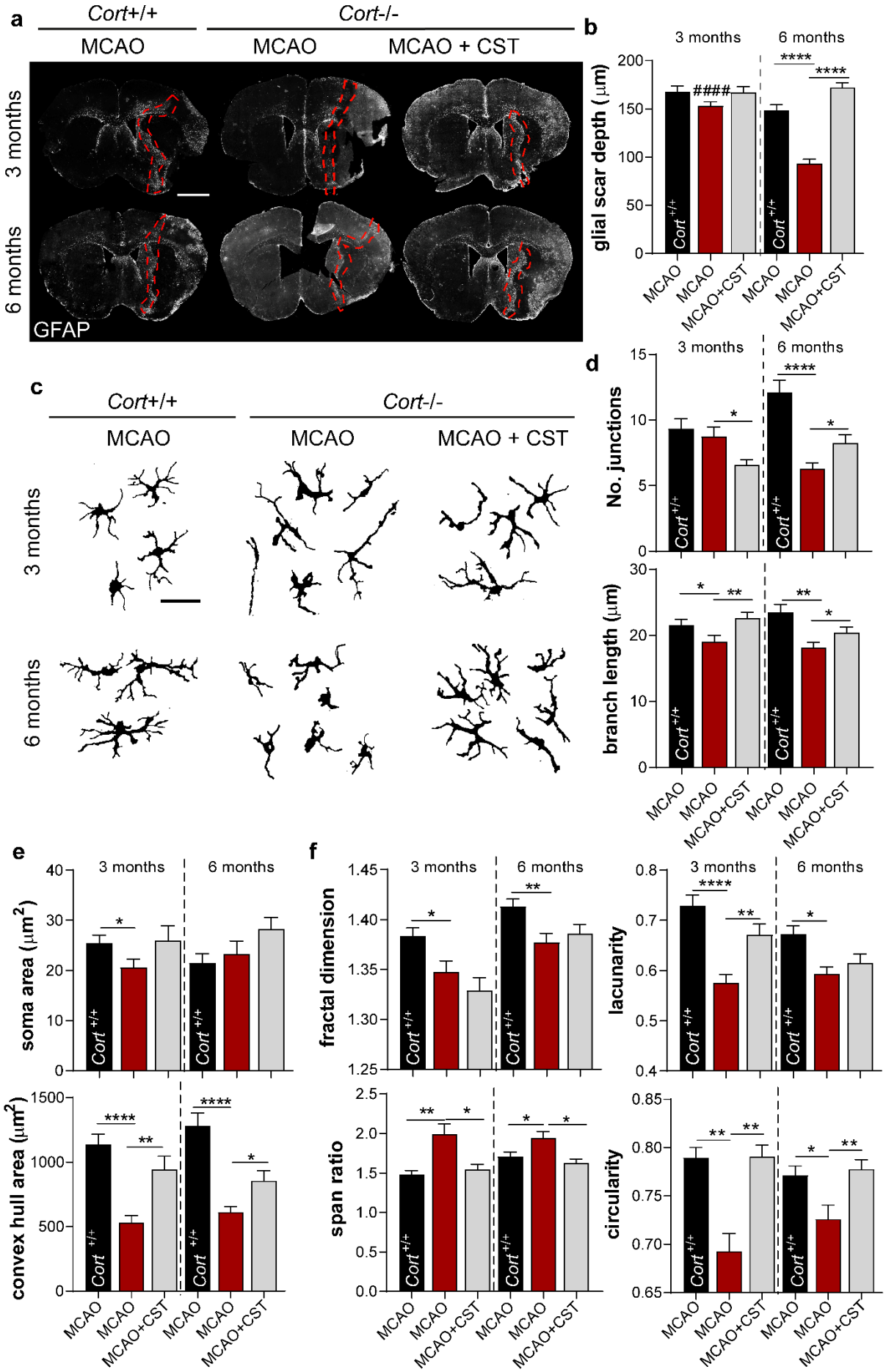
a
Cort+/+
Cort-/-
MCAO
MCAO
MCAO + CST
3 months
6 months
GFAP
b
3 months
6 months
glial scar depth (μm)
MCAO
MCAO
MCAO+CST
MCAO
MCAO
MCAO+CST
c
Cort+/+
Cort-/-
MCAO
MCAO
MCAO + CST
3 months
6 months
d
3 months
6 months
No. junctions
branch length (μm)
e
3 months
6 months
soma area (μm²)
convex hull area (μm²)
f
3 months
6 months
fractal dimension
lacunarity
span ratio
circularity

Figure 9. The deficiency of cortistatin induces impaired glial scar formation and dysfunctional astrocytes, which are modulated by exogenous cortistatin. a. Representative brain coronal sections of *Cort*$^{-/-}$ young (3 months old) and middle-aged (6 months old) mice subjected to MCAO and treated with saline solution (MCAO) or with cortistatin (115 µg/kg) (MCAO+CST) at 24 h. Sections were stained with GFAP antibody to identify astrocytes. Scale bar: 1,500 µm. Dashed red lines outline astrocyte scar. *Cort*$^{+/+}$ mice from each age group subjected to MCAO were used as controls. **b.** Glial scar depth was measured along its extent in the different experimental groups. 15-20 measures (n = 15-20) of 4-7 mice were conducted **c.** Binary images of representative astrocytes from the glial scar were analysed. Scale bar: 30 µm. **d-f.** Morphological parameters were studied. Skeleton Analysis (**d**) was used to assess the number of junctions (top panel) and their branch length (bottom panel). Soma size (**e,** top panel) was manually measured. Fractal Analysis was used to measure convex hull area (**e,** bottom panel). **f.** Fractal dimension/complexity (top left), span ratio (bottom left), lacunarity (top right), and circularity (bottom right) were also determined. Data are the mean ± SEM. Analyses were conducted on 15-20 cells from at least three independent mice. **vs Cort*$^{-/-}$MCAO, $^{\#}$*vs* the same experimental group of 6-month-old mice. $^{*/\#}p \leq 0.05$, $^{**/\#\#}p \leq 0.01$, $^{***/\#\#\#}p \leq 0.001$, $^{****/\#\#\#\#}p \leq 0.0001$.

Cortistatin deficiency is associated with enhanced BBB breakdown after stroke, which is reversed following cortistatin administration

After investigating the role of cortistatin in glial dynamics in post-ischemic stroke and given the lack of knowledge on BBB dynamics in these animals after stroke, we conducted an analysis of IgG leakage (Figure 10a). In this case, we found an increased IgG leakage in MCAO *Cort*$^{-/-}$ mice, regardless of age, compared to wild-type MCAO controls, although the differences were not significant (Figure 10b). However, cortistatin treatment significantly reduced the augmented leakage in both age groups (Figure 10b).

Regarding TJs disruption, we noted a reduction in the coverage of ZO-1, associated with an increased number of gaps in ZO-1 structure in young *Cort*$^{-/-}$ animals following MCAO compared to wild-type mice. These features were reversed by cortistatin treatment. (Figure 10c,d). Conversely, treatment in older *Cort*$^{-/-}$ mice did not influence the number of gaps, although it enhanced ZO-1 coverage (Figure 10c,d).

Furthermore, we investigated brain endothelium dynamics given the impaired peripheral endothelium already described for these mice [32]. While we observed that the vascular density was similar in young cortistatin-deficient mice compared to wild-type mice after MCAO, there was a significant reduction in the vascular density of older mice (Figure 11a,b). As observed before in wild-type mice, cortistatin treatment significantly increased the amount of vessels/area in mice lacking cortistatin. Despite not observing differences in vessel diameter in mice lacking cortistatin *vs* wild-type mice, we observed a significant greater vessel diameter after the treatment (Figure 11a,b).

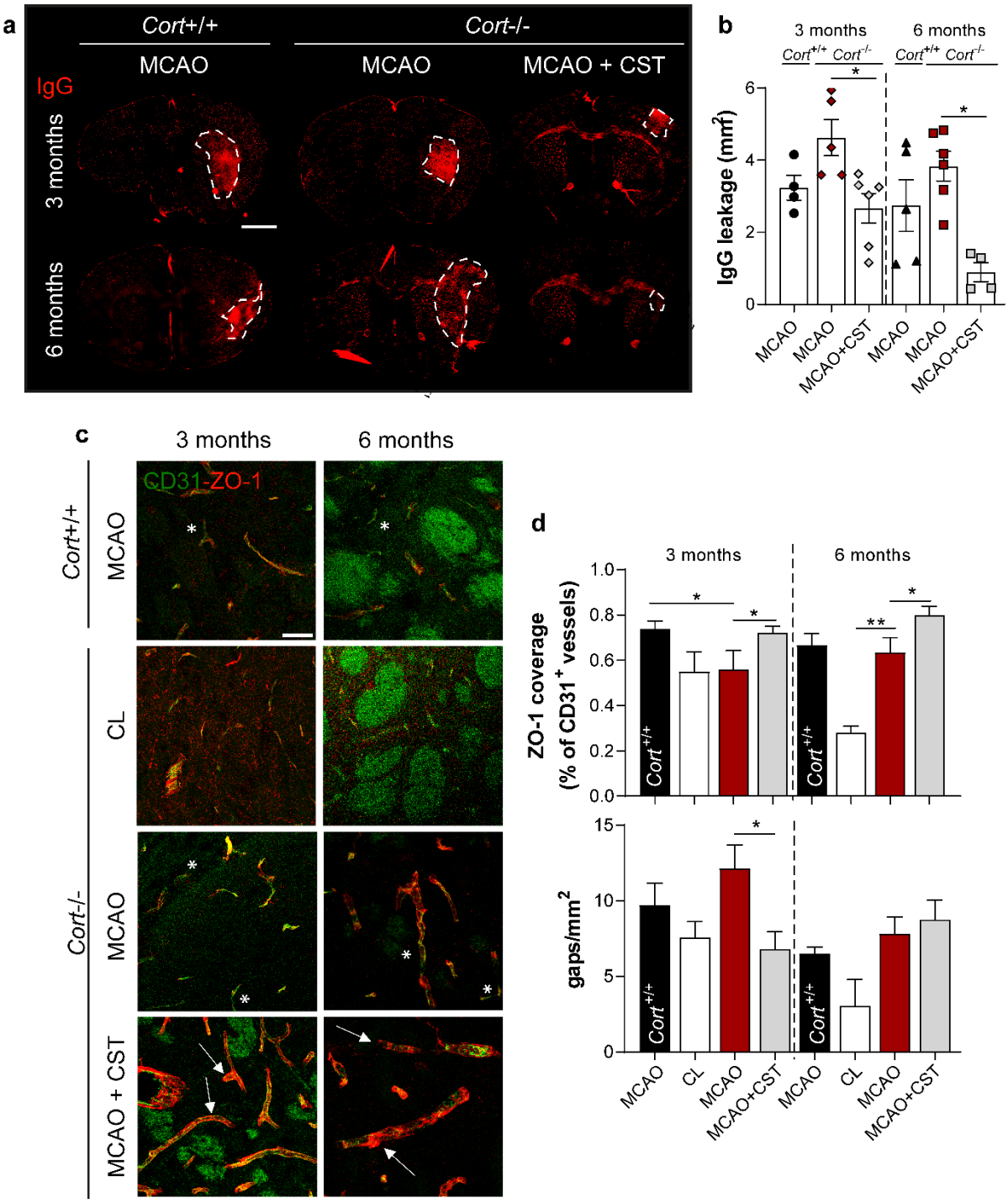

Figure 10. Cortistatin-deficient mice exhibit more severe BBB breakdown and brain endothelium disruption. a. Representative brain coronal sections of *Cort*$^{-/-}$ young (3 months old) and middle-aged (6 months old) mice subjected to MCAO and treated with saline solution (MCAO) or with cortistatin (115 µg/kg) (MCAO+CST) at 24 h. *Cort*$^{+/+}$ mice from each age group subjected to MCAO were used as controls. Scale bar: 1,500 µm. Sections are stained with a secondary antibody for IgG. IgG leakage is outlined with dashed white lines. **b.** IgG^{+} area was calculated as a measurement of IgG leakage from blood. Sections from 5-7 independent mice (N = 5-7) were analysed. **c**. Representative magnifications of the striatum of *Cort*$^{-/-}$ young (3 months old) and middle-aged (6 months old) subjected to MCAO treated with saline solution (MCAO) or with cortistatin (115 µg/kg) (MCAO+CST) at 24 h, stained with CD31 antibody for BECs (green) and ZO-1 (red) for TJs. ZO-1 gaps are highlighted with an asterisk and

ZO-1 coverage recovery with arrows). Scale bar: 30 µm. *Cort*$^{+/+}$ mice from each age group subjected to MCAO were used as controls. **d.** ZO-1 coverage (top panel) was measured as the % of positive ZO-1 area that was covering the vessel (CD31^{+} area). The number of gaps in ZO-1 structure was also determined (bottom panel). 3 different ROIs of 3-5 independent animals were analysed (N = 3-5). Data are the mean ± SEM. *vs *Cort*$^{-/-}$ MCAO, *$p \leq 0.05$, **$p \leq 0.01$.

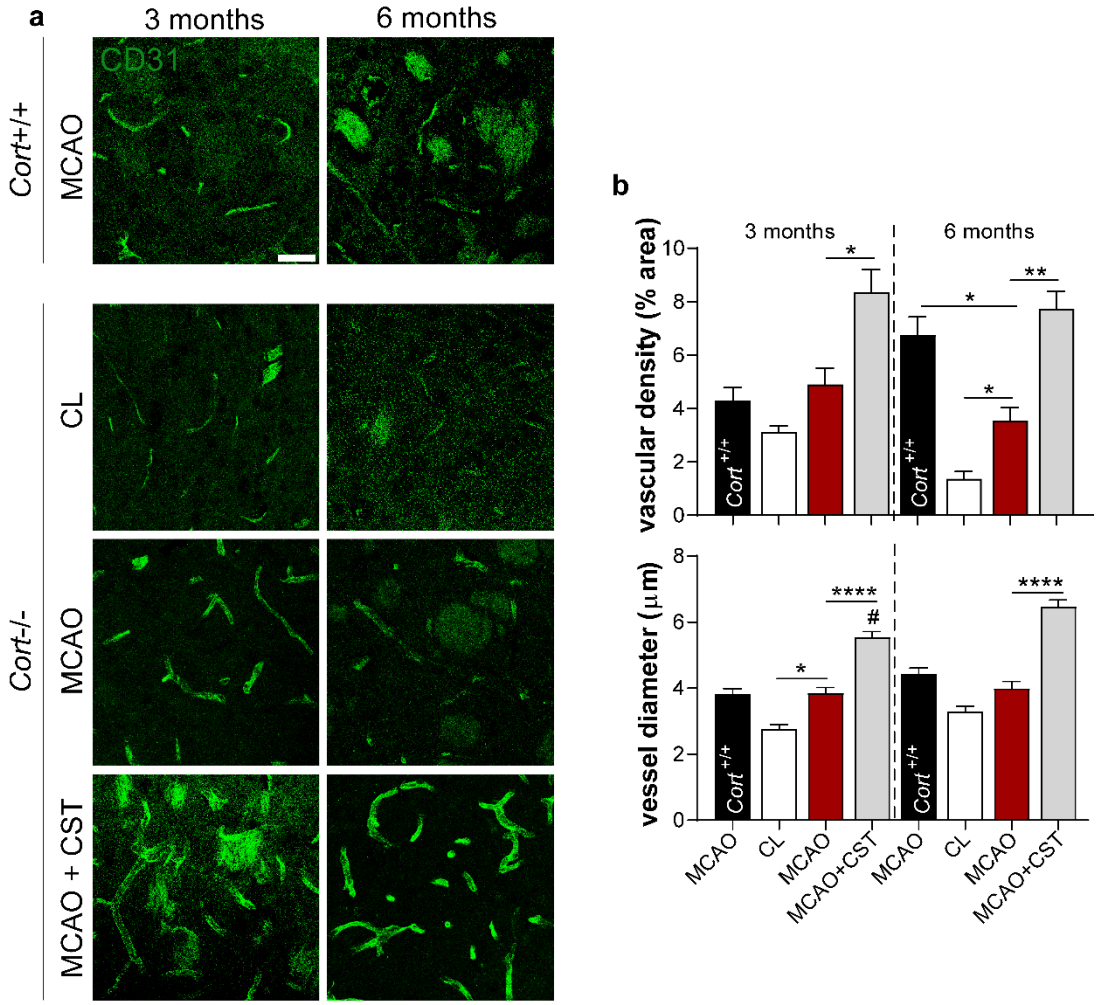

Figure 11. Impaired angiogenesis in cortistatin-deficient middle-aged mice. a. Representative images of BECs (CD31, green) from the striatum of *Cort*$^{-/-}$ young (3 months old) and middle-aged (6 months old) mice subjected to MCAO and treated with saline solution (MCAO) or with cortistatin (115 µg/kg) (MCAO+CST) at 24 h. *Cort*$^{+/+}$ mice from each age group subjected to MCAO were used as controls**.** Scale bar: 30 µm. **b.** Vascular density (top panel) was measured in the ischemic striatum or its contralateral side (CL) as the area of positive CD31 in the different experimental groups. Vessel diameter (bottom panel) was manually measured. Data are the mean ± SEM. 3 different ROIs from 3-5 mice were analysed (N = 3-5). For vessel diameter, 10-20 measures of each vessel from 5-10 vessels (n = 10-15) from each image were analysed. *vs *Cort*$^{-/-}$ MCAO, $^{\#}vs$ the same experimental group of 6-month-old mice. $^{*/\#}p \leq 0.05$, **$p \leq 0.01$, ****$p \leq 0.0001$.

Finally, given the pro-inflammatory basal state of these animals [8], and the enhanced pro-inflammatory responses in other models [11,30,33], we investigated immune infiltration and peripheral immune responses. Importantly, CD45 infiltration was enhanced in cortistatin-deficient mice after MCAO compared to wild-type in middle-aged animals but modulated after cortistatin

treatment in both age groups (Figure 12a). Regarding serum cytokines levels after MCAO, IL-6 and MCP-1 were particularly elevated in *Cort*$^{-/-}$ mice compared to control mice especially in young animals (Figure 12b). As observed in wild-type animals, older mice seemed to display an exacerbated response, although differences did not reach statistical significance (Figure 12b). Notably, treatment with cortistatin seemed to modulate IL-12, IL-6, and MCP-1, with significant differences observed in the older mice (Figure 12b). These results suggest that the pro-inflammatory context in the periphery of cortistatin-deficient mice may contribute to a more adverse response towards the ischemic insult.

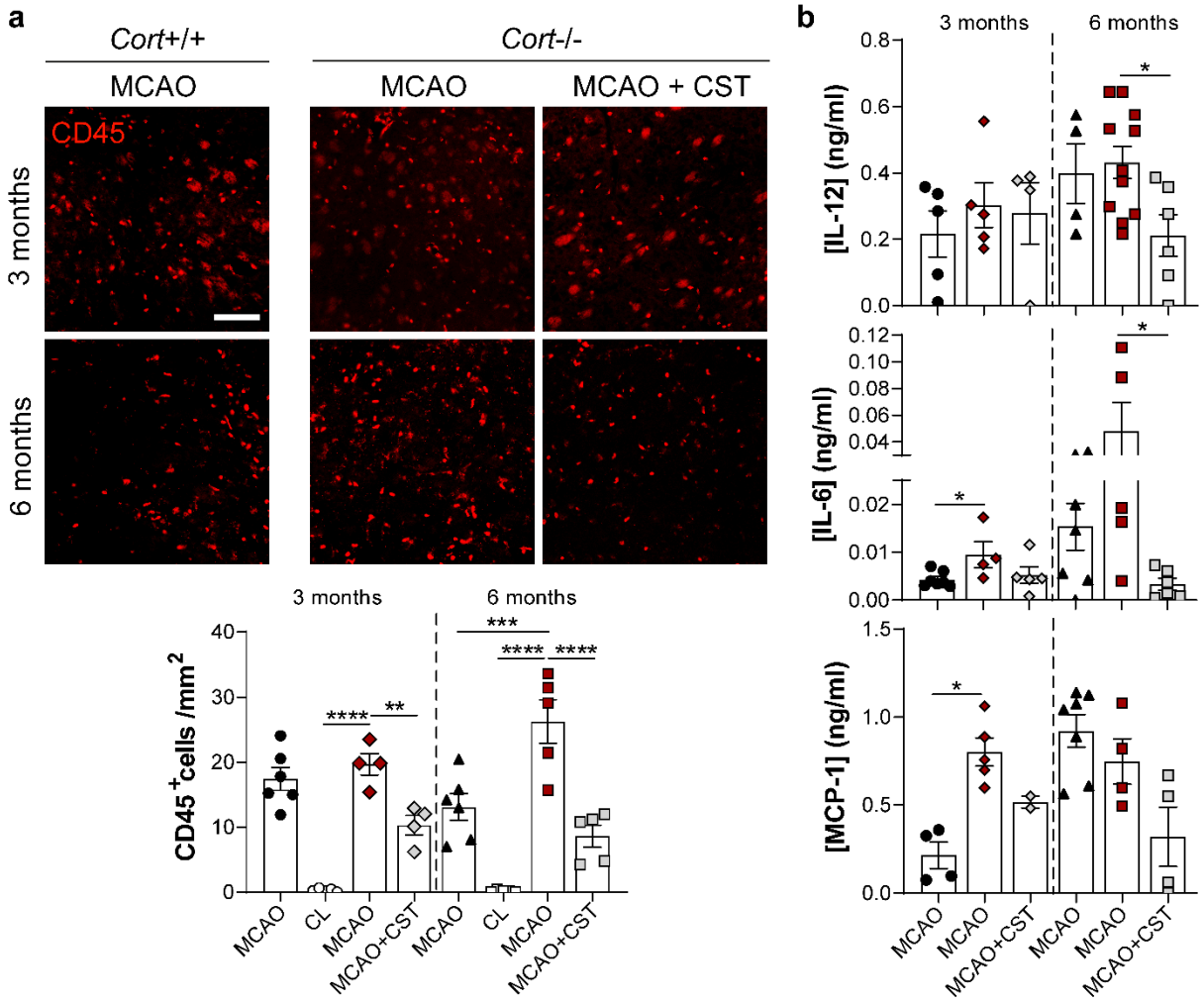

Figure 12. Deficiency of cortistatin provokes enhanced immune infiltration and altered immune peripheral response. a. Representative images of the striatum of *Cort*$^{-/-}$ young (3 months old) and middle-aged (6 months old) mice subjected to MCAO and treated with saline solution (MCAO) or with cortistatin (115 µg/kg) (MCAO+CST) at 24 h. *Cort*$^{+/+}$ mice from each age group subjected to MCAO were used as controls. Sections were stained with CD45 antibody for leukocytes (top panel)**.** Scale bar: 100 µm. Leukocyte density (number of cells/mm^2) was calculated in the striatum and in the contralateral side (CL) of the different experimental groups (bottom panel). **b.** IL-12, IL-6, and MCP-1 concentration (ng/ml) measured in serum by ELISA assay. Data are the mean ± SEM. N = 4-6 independent mice. **vs Cort*$^{-/-}$ MCAO *$p \leq 0.05$, **$p \leq 0.01$, ***$p \leq 0.001$, ****$p \leq 0.0001$.

In summary, after MCAO *Cort*$^{-/-}$ mice displayed a more severe neurological deficit, dysfunctional microglia and astrocyte response, together with a disrupted BBB that leads to increased leakage and immune infiltration. Moreover, the immune peripheral response is enhanced compared to wild-type mice. The administration of exogenous cortistatin after stroke to mice lacking cortistatin, regulates BBB breakdown and local and peripheral immune response. Despite the effect of cortistatin being exerted in a different way than when administered in MCAO wild-type animals, it also leads to decreased neurodegeneration and neuroinflammation. Remarkably, the beneficial effect of cortistatin affects both young and middle-aged animals.

DISCUSSION

The pathogenesis of stroke is a highly intricate process in which various types of nervous, circulating, and cerebral immune cells exert profound dual roles depending on their cell context, spatial location, and timing. The complexity of this pathophysiology presents a significant challenge in designing therapeutic approaches, contributing to stroke remaining the second leading cause of death worldwide. Therefore, gaining a deeper understanding of the intricate relationship between the nervous, vascular, and immune systems is essential for improving stroke prognosis. In this context, we propose that the neuropeptide cortistatin, a crucial link between the CNS and the immune system, with anti-inflammatory, neuroprotective, and immunomodulatory properties, could function as an endogenous pleiotropic key mechanism in the pathophysiology of ischemic stroke, as well as a potential therapeutic agent. To test this hypothesis, we initially explored the potential therapeutic properties of this neuropeptide in a preclinical model of stroke (MCAO) at later stages (*i.e.,* 24 h), aiming to extend the current therapeutic window (4-6 h for the rtPA). Moreover, we conducted the model in wild-type and cortistatin-deficient mice following cortistatin administration, to examine the endogenous role of this neuropeptide.

First, it is important to highlight that one of the reasons for the failure in translating bench-to-bedside findings is the exclusion of risk factors such as atherosclerosis or aging. Aging, in particular, is a significant non-modifiable factor, not only serving as a risk factor but also being linked to increased vulnerability and reduced capacity to recover from brain injury [34]. Despite this, most studies are currently conducted in young animals, leaving the impact of aging relatively unexplored. To account for the age-related factor, we performed the aforementioned experiments using both young (3 months old) and middle-aged mice (6 months old). Typically, older animals (15-24 months old) are employed to study the aging component in stroke [35,36]. However, cortistatin-deficient mice already manifest an elevated susceptibility to various injury models [8,11,30,33,37], as well as a premature aging-like phenotype that is evident as early as 6 months (unpublished data from the lab). Consequently, the use of older animals might have compromised the success of the model due to the potential high mortality of these animals. Moreover, it is important to note that the incidence rates in people under the age of 70 have worryingly risen in

the last 20 years, accounting for 63% of strokes. Therefore, studies conducted in middle-aged are also of great relevance.

Another reason contributing to translational failure is the use of treatments focused on a sole mechanism, or the emphasis on irrelevant therapeutic windows, often focusing on the hyper-acute phase to fall into the range of rtPA, or slightly later without distinguishing between phases. In this sense, neglecting the complex, spatio-temporally variable nature of stroke pathophysiology has led to poor prognosis in many cases [3]. Therefore, we advocate that the focus should be on cytoprotective factors that target different aspects of the ischemic cascade in the later stages of stroke. This approach would provide a broader treatment window, allowing for the enrolment of a substantial number of patients. Therefore, we examined the immediate effect of the neuropeptide at later stages (24 h) to investigate whether this neuropeptide could exert beneficial effects beyond the currently limited time frame. To collectively examine the potential effect of the neuropeptide, we evaluated neurodegeneration, glial population dynamics, BBB breakdown, brain vasculature alterations/regenerative process, and immune response 48 h following MCAO.

Our findings showed that cortistatin treatment at later stages reduced lesion sizes, but did not show a significant improvement in the neurological score of wild-type mice. These non-significant differences in score, despite an evident reduction in the neuronal lesion, may be attributed to the use of a mild rather than a severe stroke model. Indeed, in the mild model, clinical manifestations are very similar between low scores, making it challenging to observe the correlation between infarct volume and scores [38]. Nevertheless, mild models also induce less damage and reduced endothelial lining injury [39]. Importantly, cortistatin-deficient mice exhibited worsened neurological scores in both age groups compared to wild-type mice. Accordingly, higher susceptibility of cortistatin-deficient mice has been observed in other injury models [8,11,33,40]. Importantly, cortistatin treatment reduced neurological scores in cortistatin-deficient young and middle-aged mice. The capacity of cortistatin to regulate neurological deficits in older mice or those more susceptible to stroke, which present severe clinical manifestations (*i.e.,* cortistatin-deficient mice), is highly promising.

On a different note, the major immediate consequence of acute stroke is irreversible neuronal cell death and brain damage [39]. Particularly, ischemic stroke in humans and the MCAO model in rodents are characterized by an ischemic core and a distinguishable penumbra [41]. Interestingly, despite no significant impact on neurological deficits, cortistatin treatment did reduce the lesion size, especially targeting the core and the penumbra, in wild-type animals from both age groups (Figure 13). Importantly, cortistatin treatment seemed to target the viability of dendritic processes and neuron bodies, as reported by both CV and MAP-2 staining. Notably, beyond the traditional CV staining, MAP-2 offers a more accurate insight into the initial stages of neuron death even if the process is not complete yet, which in turn offers potential opportunities for intervention [42]. In this sense, the reduced lesion size observed in the striatum following cortistatin treatment with MAP-2

staining indicates that cortistatin efficiently targets these initial critical stages of neuronal death, while also protecting neuronal bodies.

Conversely, despite exhibiting poorer neurological deficits, cortistatin-deficient animals did not exhibit more severe lesions than wild-type counterparts. In this line, our results conform to other studies reporting that infarct size does not always correlate with neurological function and functional outcomes [39,43,44]. This suggests that the evaluation of stroke outcomes should not solely rely on ischemic volumes. Notably, no differences were either observed between young and middle-aged animals in any of the genotypes. Despite this being surprising, several studies in rodents and humans have reported that aging is not necessarily correlated to developing a larger infarct size, even if aged individuals recover less effectively than younger ones [44,45]. This may be attributed to the fact that, although the timing of neuronal loss in aged animals is accelerated, the process of neuronal degeneration ultimately converges on a similar endpoint in young and old individuals [44]. This would explain the lack of differences between young and middle-aged mice, both in wild-type or cortistatin-deficient mice. Hence, we advocate that the reductions in ischemic lesions by cortistatin in both age groups and genotypes are of particular interest and value.

The neuroprotective effects of cortistatin agree with previous investigations conducted by our group and others, where we demonstrated that cortistatin treatment exerts a protective effect over the neurons from the substantia nigra pars compacta and the striatum of a mouse model of Parkinson's disease [12]. Besides, cortistatin has been reported to protect dopaminergic neurons in mesencephalic cultures exposed to the MMP toxin [12], and primary cortical neurons following β-amyloid intoxication [46]. However, the precise mechanisms underlying the influence of cortistatin in neurological lesions are not fully understood (*i.e.,* whether it directly inhibits apoptosis, neuronal degeneration, oxidative damage, or a combination of these factors). Accordingly, the questions of whether cortistatin exerts a direct neuroprotective effect on neurons or if, conversely, it is exerting other responses (*i.e.,* anti-inflammatory, immunomodulatory effects) on different cells, indirectly benefiting neurons, stand and remain a possibility that cannot be discarded.

For decades, ischemic stroke research has primarily focused on rescuing neurons in the penumbra region to prevent the expansion of the infarct core. However, it is now evident that excitotoxicity, oxidative stress, neuroinflammation, or peripheral immune response can contribute to secondary neuronal cell death [309], becoming increasingly clear that solely focusing on neuronal death would be oversimplistic [294]. Therefore, this study aims to explore additional potential roles of cortistatin in stroke pathophysiology, particularly elucidating its impact on the neuroinflammatory response.

In the first hours following ischemic stroke, microglia rapidly respond and accumulate in the infarct core and the peri-infarct zone [47]. In this sense, our observations revealed an enhanced number of microglia in the ischemic core following cortistatin treatment in wild-type mice in both age groups, suggesting potential involvement in the phagocytosis of dead neurons, as a clearly

reduced area of neurological lesion was found in treated-mice. Interestingly, an elevated number of microglial cells was found also in MCAO cortistatin-deficient middle-aged mice compared to wild-type, which was unaltered following cortistatin treatment (Figure 13). Whether the phagocytic function of microglia in stroke is advantageous or detrimental remains uncertain, emphasizing the importance of maintaining a delicate balance for an improved stroke prognosis. Specifically, some studies reported that enhancing the phagocytic capability of microglia in a MCAO model can foster efficient clearance of tissue debris [48], while others report that hyperreactive microglia can engulf live or stressed neuronal cells and result in worsened neurological deficits [49]. Notably, previous studies from our group (data not shown) have demonstrated that while wild-type microglia produce neurotrophic and regenerative mediators, and efficiently eliminate debris, cortistatin-deficient microglia exert deficient phagocytosis in physiological and demyelinating environments [50]. This supports the idea that the increased number of microglia in the ischemic core of cortistatin-treated wild-type mice would be efficiently phagocyting dead cells. On the contrary, although elevated density was also found in cortistatin-deficient animals, this would be likely a compensatory effect, since microglia would not be as efficiently involved in phagocytosis.

While most microglia are engaged in engulfing dead neurons in the ischemic core, those in the peri-infarct area exhibit a different phenotypic polarization into either protective or detrimental forms, depending on surrounding factors [51,52]. The initially predominant microglia, characterized by phagocytosis, reduced production of inflammatory factors, and enhanced neuroprotective factors, is temporary and gives way to more pro-inflammatory and less phagocytic microglia in the chronic phases, ultimately impairing axon regrowth [52]. Traditionally, this process has been characterized based on basic metrics such as long processes, indicating ramified homeostatic microglia, or short processes indicating reactive microglia. Nevertheless, microglia undergo changes across multiple scales following injury (*e.g.,* branch configuration, degree and length of branching, soma size and shape, diameter, cell territory, cytoskeletal organization, relative cytoplasmic volume, membrane configuration, and receptor distribution), that goes far beyond the oversimplified paradigm of M1/M2 or ramified/ameboid dichotomy [53]. To address these features, different tools to quantitatively address morpho-function and to precisely assess morphological features of microglia (*e.g.,* Fractal Analysis or Skeleton Analysis) can be employed. Importantly, these analyses serve as a starting point, and further studies integrating function, morphology, transcriptome, metabolome, and proteome, through high-dimensional techniques should be conducted [54].

In our study, several parameters related to branching, soma volume, complexity, or lacunarity collectively showed marked reactive microglia after MCAO in wild-type mice, regardless of age. Interestingly, microglia from both age groups behaved differentially after cortistatin treatment, with microglia shifting to a more homeostatic state in middle-aged mice (Figure 13). Similar to the effect on lesion size, the more pronounced modulation of microglia by cortistatin in older animals holds promise for targeting a broader age range, potentially benefiting the elderly. This modulation of

microglia morpho-function also conformed with previous results from our group and others in other neuroinflammatory models (*i.e.,* Multiple Sclerosis, Parkinson's, and sepsis) [8,12,55]. These studies reported that microglia seemed to return to a homeostatic ramified-like state after cortistatin treatment, which was markedly correlated with a better prognosis of the disease. Notably, although young wild-type and cortistatin-deficient microglia displayed a similar phenotype after stroke in our study, we observed hyper-ramified microglia in middle-aged *Cort*$^{-/-}$ mice compared to wild-type and their respective young mice (Figure 13). Interestingly, other studies have reported hyper-ramification of microglia in response to acute and chronic stress and excitotoxicity, a response that might be implicated in synaptic modifications [56,57]. This is in line with the stress-like behaviour exhibited by these animals [8] and may imply hyperreactivity of these cells prior to ischemia, negatively impacting subsequent neurological damage. Accordingly, other studies from the group reported exacerbated inflammatory responses in cortistatin-deficient microglia [8]. Importantly, cortistatin treatment modulated this phenotype, resembling microglia found in MCAO wild-type mice in some properties while mirroring the microglia observed in healthy wild-type animals in most of the parameters. This suggests that in cortistatin-deficient animals, cortistatin may modulate microglia reactivity differently compared to wild-type mice, effectively reversing its dysfunctional phenotype.

Numerous questions surrounding the transitions between the different microglial subsets remain unanswered, and the specific molecular cues prompting this transition are yet to be identified [39]. In this sense, our study suggests that cortistatin could be one of these important factors. In particular, cortistatin may be capable of regulating microglia proliferation towards a more phagocyting and protective-like phenotype, while modulating the transition of reactive pro-inflammatory-like microglia to a more protective-like state in the penumbra. However, sustained reactivity of microglia over time is not beneficial either. As our study and others have reported [8,58,59], treatments in the later stages have demonstrated that shifting microglia towards a more anti-inflammatory phenotype contributes to the recovery processes. Accordingly, our research demonstrates that the detrimental outcomes of microglia reactivity are clearly counterbalanced by beneficial effects, including phagocytosis and the release of trophic factors. Further studies will address the exact mechanisms through which cortistatin-modulated microglia can exert this immunomodulatory role.

Beyond microglia, astrocytes greatly contribute to the neuroinflammatory response. After ischemic damage astrocytes proliferate and migrate, creating a barrier around the edges of severely damaged tissue from the surrounding viable neural tissue [60]. Notably, the molecular and cellular mechanisms that underlie the formation of the glial scar and astrocyte reactivity are not completely understood. These likely involve a complex and balanced interplay of molecular signals that can simultaneously boost phagocytosis and debris clearance, which would be essential for the protection and conservation of the still-healthy tissue [60–62]. Similar to microglia, an A1/A2 paradigm for astrocyte morphology and function has been proposed [63]. However, the

spatiotemporal heterogeneity of reactive astrocytes has demonstrated that this classification is too simple and highly questionable, so additional parameters far from traditional approaches should be considered.

In this research, we observed that cortistatin treatment enhanced the thickness of the glial scar in young and middle-aged animals. After conducting quantitative analyses of the morpho-function of these astrocytes forming the glial scar, we observed a reactive phenotype. The thicker glial scar produced by these astrocytes may be closely related to the observed protection of the neuronal tissue. Surprisingly, we described an impaired glial scar formation in cortistatin-deficient mice in both age groups (Figure 13). Interestingly, although very scarce, these astrocytes display a completely different phenotype from wild-type mice after stroke, exhibiting small, non-ramified, elongated forms, not previously described in the bibliography. Interestingly, these results did not align with previous descriptions from astrocytes in cortistatin-deficient mice in other neuroinflammatory models, such as EAE [8] or Parkinson's [12]. In detail, these studies showed no impaired response of astrocytes in cortistatin-deficient mice, rather, an upregulated astrogliosis was observed, which was reversed by cortistatin treatment. However, it is interesting to note that in these models, damage was evaluated at chronic stages, where the astrocyte response might be chronic and detrimental. Therefore, the most beneficial response in stroke at this stage would be to enhance the astrocytic response, as the underlying astrocytes would likely adopt a protective phenotype towards neurons. Accordingly, defective astrocyte scar formation in various transgenic loss-of-function models of ischemia has been shown to result in increased lesion size, demyelination, and death of local neurons, leading to decreased recovery of function [61,62,64]. Nevertheless, it is important to mention that uncontrolled astrogliosis and excessive scar formation over time may ultimately be harmful (*e.g.,* exacerbating inflammation or interfering with synapse sprouting or axon growth during the recovery phase). Future studies would address the role of cortistatin in modulating such response at later stages.

On the other hand, BBB breakdown stands out as a primary hallmark of stroke, manifesting shortly after artery occlusion and persisting for several days to weeks [65]. However, the conventional classification of BBB alterations after stroke is again too simple and restricted to "opening" or "closing" (*i.e.,* "bad" or " good") being this dichotomy completely outdated. Instead, BBB permeability exhibits a multiphasic pattern across various stroke stages (*i.e.,* hyperacute, acute, subacute, and chronic stages), each associated with distinct biological events [66]. In this study, we have focused on its acute phase, where the permeability is at its highest, and neuroinflammatory response can aggravate the injury [66]. Notably, our findings revealed an increased IgG leakage after stroke in wild-type animals, being slightly more pronounced in cortistatin-deficient animals (Figure 13). This observation is consistent with the increased BBB leakage previously reported by our group in a model of mild neuroinflammation induced by bacterial LPS, that also courses with BBB disruption [13]. Interestingly, cortistatin-deficient mice exhibited BBB disruption even under physiological conditions, confirming the great susceptibility of the barrier

of these animals. Remarkably, the treatment with cortistatin mitigated this increased leakage, especially in cortistatin-deficient mice, and could therefore be an important therapeutic advantage for this severe complication [13]. The disruption of the BBB is generally linked to endothelial damage and disrupted TJs and AJs. In this sense, we focused our study on the endogenous and therapeutic role of cortistatin in endothelial dynamics after ischemic injury and reperfusion. We found that cortistatin-deficient mice exhibited more gaps in ZO-1 structure after MCAO, when compared to their wild-type counterparts. Notably, cortistatin treatment could reduce this enhanced number of gaps This aligns with previous results where we demonstrated that BECs isolated from cortistatin-deficient mice exhibited both a disrupted BBB endothelium in homeostatic conditions, exacerbated after ischemic damage (*i.e.,* enhanced permeability, TJ-AJs disruption, increased pro-inflammatory state). Importantly, the exogenous addition of cortistatin reversed all these features (Figure 13) [13].

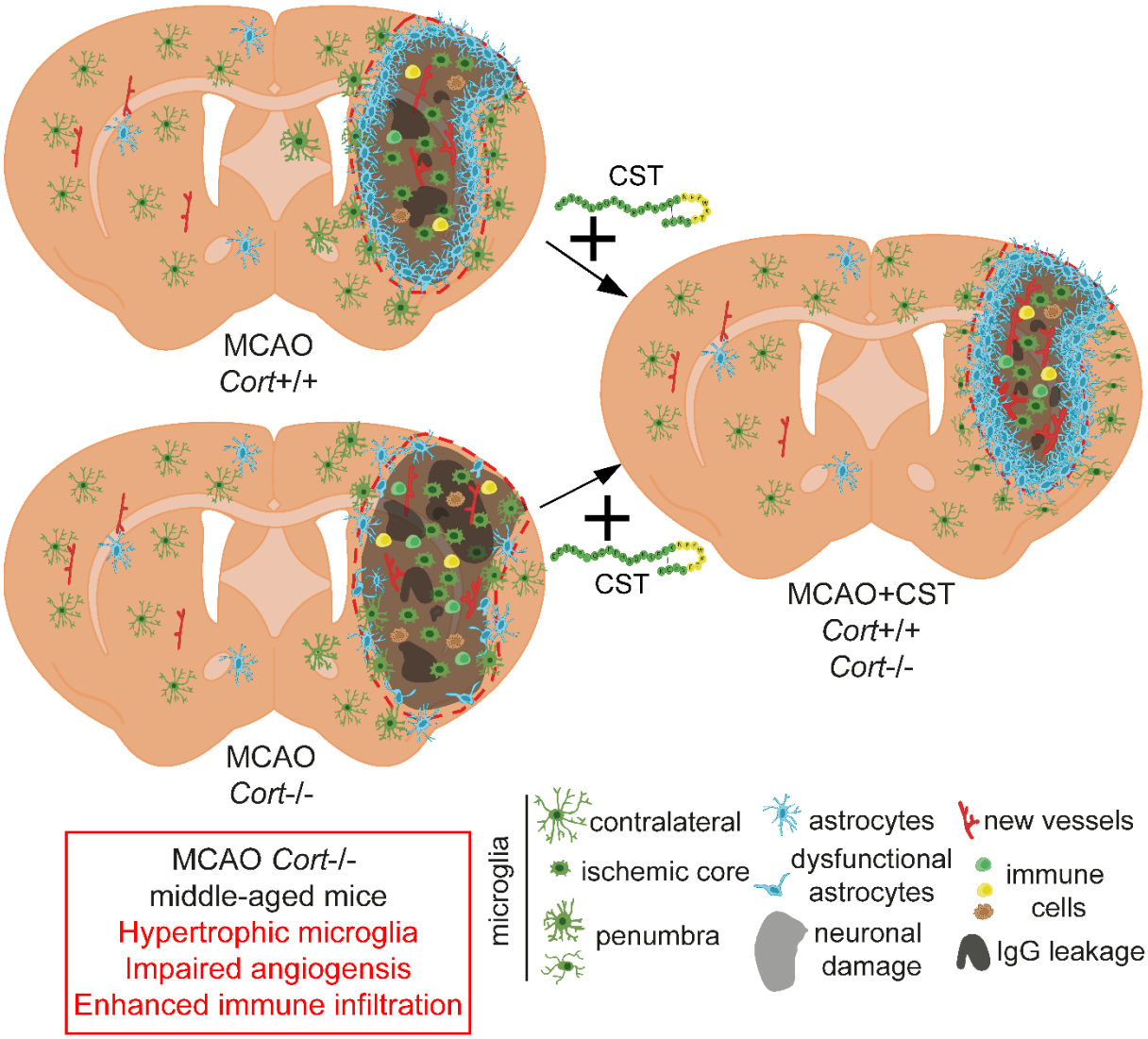

Figure 13. Schematic illustration of the proposed role of cortistatin in stroke pathophysiology 48 h after the onset. Top left, wild-type mice response after stroke, *i.e.,* neuronal mild damage, microglia proliferation in the ischemic core (grey shadow), microglia reactivity in the penumbra (dashed

red lines), astrocyte scar formation, mild BBB leakage, immune infiltration, and angiogenesis promotion. **Bottom left**, deregulated response after stroke of cortistatin-deficient mice, *i.e.,* severe neurological damage, microglia proliferation in the core, hyper-ramified microglia in the penumbra, enhanced BBB disruption, impaired glial scar, elevated immune infiltration, and deregulated angiogenesis. **Right**, cortistatin treatment reversed all the mentioned deficits in both conditions, *i.e.,* reduces neurological damage, enhances microglia proliferation in the core, regulates protective microglia in the penumbra, increases glial scar formation, reduces BBB leakage and immune infiltration, and promotes angiogenesis.

Finally, it is crucial to acknowledge that a stroke is a complex process that not only concerns the brain but also peripheral tissues organism-wide. Shortly after the interruption of CBF and the subsequent hypoxia, ECs express selectins in response to oxidative damage, quickly engaging circulating innate immune cells, and triggering the rapid pro-inflammatory response in the periphery [2]. Moreover, the degradation of BBB components facilitates the extravasation of these cells, at different time intervals and with variable cadences. Our investigation shows that cortistatin modulates immune infiltration in the brain of both wild-type and cortistatin-deficient mice in both age groups (Figure 13). Similar effects of cortistatin treatment were found by our group in an EAE model [8] and in a BBB *in vitro* model, where we observed that cortistatin can modulate the transmigration of macrophages and T cells across the endothelium [13]. To what extent cortistatin is involved in regulating adhesion molecules, whether is directly affecting immune cells instead, or both, are subjects that we cannot fully elucidate at this point. In fact, cortistatin exerts immunomodulatory activities in activated macrophages *in vitro,* suggesting that we cannot dismiss the latter [67]. As highlighted when addressing the neuroinflammatory response, we again advocate that understanding each specific mechanism at each specific stage seems to be paramount to achieving a better modulation of the overall response.

Beyond periphery-only effects, the elevation of inflammatory mediators following ischemia occurs both centrally and peripherally [68]. Circulating cytokines produced by the glial niche in response to ischemic injury reach the systemic circulation and trigger the immune response in lymphoid organs, increasing the production of inflammatory mediators in circulating and splenic immune cells [29]. In general, an increased production of pro-inflammatory cytokines and a decreased production of anti-inflammatory cytokines are correlated with poorer clinical outcomes and larger infarct size in animal models [69]. In this sense, we observed an enhanced pro-inflammatory response (*i.e.,* IL-6, IL-12, MCP-1) in middle-aged mice compared to young animals, likely associated with an aging-related factor. Moreover, these factors were significantly reduced after cortistatin treatment in both age groups, underlining the endogenous role of cortistatin as a mediator/brake in excessive inflammation, together with its potent anti-inflammatory properties when used as therapy. Importantly, elevated levels of IL-6 and IL-12 in serum within the first 24 h following a stroke have been associated with a decline in the functional state of patients [70–72]. Similarly, MCP-1 expression becomes enhanced in the ischemic penumbra, cerebrospinal fluid, and serum after stroke, and positively correlates with lesion enlargement [73,74]. Nevertheless, the Janus-faced nature of peripheral inflammation cannot be dismissed (*i.e.,* the same factors may

either contribute to tissue damage or protection, depending on the temporal-spatial context of their expression [75]). For example, IL-6 serves as a neurotrophic factor in the late phase, improving functional outcomes, reducing stroke volume in mice [76], and promoting angiogenesis after stroke [75]. Hence, considering the dual role of cytokines in both the acute and the recovery phases, complete blockade could lead to undesired effects [77]. In this context, it is important that cortistatin modulated, rather than completely reduced, the levels of these cytokines/chemokines. Besides, it is crucial to consider that these experiments were conducted in the acute phase, where cytokines typically exert a pro-inflammatory/detrimental function. Future studies should address the dynamics of cortistatin regulation over cytokines and chemokines production in later stages.

The complex interplay between the CNS and the immune system is possible thanks to the presence of a biochemical common language of neurotransmitters, neuropeptides, and hormones. In addition to this investigation, previous studies have long demonstrated the protective effect of neuropeptides in stroke. Over two decades ago, a study demonstrated a reduction in lesion size in rats following treatment with somatostatin, octreotide, and cortistatin in a permanent MCAO model at seven days [78]. However, the exact mechanisms underlying this effect were not elucidated, and no subsequent studies have further investigated cortistatin. Additionally, various studies have demonstrated that ghrelin administration reduces the infarct volume and improves neurological deficits and BBB breakdown in a MCAO model in rats [79,80]. Interestingly, elevated levels of ghrelin in serum have been found after stroke, probably as a compensatory neuroprotective effect against ischemia [81,82]. Accordingly, cortistatin expression was also found elevated in various vascular disorders (*e.g.,* mouse arteries exposed to blood-flow alterations, in plasma of patients with coronary artery lesions, and in the hearts of mice with autoimmune myocarditis [32,83]), indicating a potential compensatory mechanism in response to acute injuries. Interestingly, cortistatin and somatostatin levels were also enhanced in the penumbra during the early stages of stroke in mouse models, while being strongly decreased in the ischemic core [84]. Similarly, we previously found that BECs from mice and humans showed decreased cortistatin levels upon oxygen-glucose deprivation injury [13]. Remarkably, levels of cortistatin were also impaired in the temporal lobule of Alzheimer's disease patients [85] or in the retina of patients with diabetic retinopathy [86]. These findings suggest that while neuropeptide levels may initially rise in the acute phase of damage, they subsequently decrease in chronic stages, correlating with a poorer prognosis. Restoring neuropeptide levels, especially in chronic neurodegenerative/neuroinflammatory disorders, could serve as a novel neuroprotective mechanism. Future studies will explore whether dynamic changes in these neuropeptides could also act as biomarkers for predicting the prognosis of stroke or other neuroimmune conditions.

Gaining a deeper understanding of the interplay between the structure and function of neuropeptides and their receptors both in physiological and pathologic contexts, holds the key to developing innovative pharmacological agents [87]. In this context, cortistatin is known to bind to somatostatin, ghrelin, and Mgrx2 receptors, as well as to others yet unknown. However, the exact

molecular mechanism through which cortistatin acts through their receptors exerting protective properties in stroke is still unknown and further studies should address this question. Probably, the potential capability of cortistatin to synergistically signal through somatostatin/ghrelin receptors (in addition to a yet unknown specific receptor) could confer an advantage over the individual regulation of stroke pathophysiology exerted by somatostatin/ghrelin. Moreover, the intriguing possibility that cortistatin exerts its mechanisms through different cell types (*i.e.,* neurons, microglia, astrocytes, pericytes, BECs, or immune cells) could also confer an advantage against other potential therapeutics.

In conclusion, cortistatin stands as a pleiotropic endogenous key factor and a potential therapeutic agent in stroke management. In particular, its capacity to concurrently modulate several pathological features, such as clinical manifestations, neurological damage, glial over-reaction, astrocyte scar, or BBB breakdown holds significant promise compared to interventions targeting only a single aspect. Furthermore, cortistatin emerges as a critical factor modulating the intricate interplay between the CNS and the immune system, regulating exacerbated cellular and molecular responses from both systems that could impact brain homeostasis. Finally, its efficient application at later times and across different ages and phenotypes could open the door for extending a therapeutic time window, which is unfortunately very narrow or non-existent for many patients who do not meet the clinical criteria. The useful insights derived from this study have the potential to contribute to the development of novel therapeutic strategies not only for stroke, but also for other CNS pathologies associated with BBB dysfunction, glial over-reactivity, or impaired CNS-immune system interplay

ACKNOWLEDGEMENTS

The authors would like to thank the Animal Care Unit and Microscopy Service Unit staff from IPBLN for the technical support.

FUNDING

This work was supported by the Spanish Ministry of Economy and Competitiveness (MCIN)/Spanish Research Agency (AEI)/10.13039/501100011033 grants: SAF2017-85602-R (to E.G-R.), FPU-program FPU17/02616 (to J.C-G.), FPI-program PRE2018-084824 (to I.S-M.) and PRE2021-100172 (to P.V-R.), the Swiss Science Foundation FNS 310030_212233 grant to L.H, and the European Molecular Biology Organization EMBO-STFL8942 grant to J.C-G.

CONTRIBUTIONS

EG-R conceived, design and supervised the whole study. J.C-G and E.G-R outlined the experiments and analysed all the data. J.C-G, L.B, P.V-R, I.S-M, and I.F-L performed the experiments. J.C-G, L.B, M.P, P.H-C, L.H, and .EG-R interpreted the data, and discussed the results. J.C-G and E.G-R wrote and revised the manuscript. All authors have read and agreed to the published version of the manuscript.

BIBLIOGRAPHY

1. Translational Research in Stroke. In: Lapchak PA, Yang G-Y, editors. Singapore: Springer Singapore; 2017.

2. Campbell BCV, De Silva DA, Macleod MR, Coutts SB, Schwamm LH, Davis SM, et al. Ischaemic stroke. Nat Rev Dis Primers. 2019;5:1–22.

3. Drieu A, Levard D, Vivien D, Rubio M. Anti-inflammatory treatments for stroke: from bench to bedside. Ther Adv Neurol Disord. 2018;11:1756286418789854.

4. Delgado M, Gonzalez-Rey E. Role of Cortistatin in the Stressed Immune System. In: Savino W, Guaraldi F, editors. Frontiers of Hormone Research. S. Karger AG; 2017. p. 110–20.

5. de Lecea L, Criado JR, Prospero-Garcia O, Gautvik KM, Schweitzer P, Danielson PE, et al. A cortical neuropeptide with neuronal depressant and sleep-modulating properties. Nature. 1996;381:242–5.

6. Córdoba-Chacón J, Gahete MD, Pozo-Salas AI, Martínez-Fuentes AJ, de Lecea L, Gracia-Navarro F, et al. Cortistatin is not a somatostatin analogue but stimulates prolactin release and inhibits GH and ACTH in a gender-dependent fashion: potential role of ghrelin. Endocrinology. 2011;152:4800–12.

7. Deghenghi R, Papotti M, Ghigo E, Muccioli G. Cortistatin, but not somatostatin, binds to growth hormone secretagogue (GHS) receptors of human pituitary gland. J Endocrinol Invest. 2001;24:RC1-3.

8. Souza-Moreira L, Morell M, Delgado-Maroto V, Pedreño M, Martinez-Escudero L, Caro M, et al. Paradoxical Effect of Cortistatin Treatment and Its Deficiency on Experimental Autoimmune Encephalomyelitis. J Immunol. 2013;191:2144–54.

9. Chiu C-T, Wen L-L, Pao H-P, Wang J-Y. Cortistatin Is Induced in Brain Tissue and Exerts Neuroprotection in a Rat Model of Bacterial Meningoencephalitis. J Infect Dis. 2011;204:1563–72.

10. Braun H, Schulz S, Becker A, Schröder H, Höllt V. Protective effects of cortistatin (CST-14) against kainate-induced neurotoxicity in rat brain. Brain Res. 1998;803:54–60.

11. Falo CP, Benitez R, Caro M, Morell M, Forte-Lago I, Hernandez-Cortes P, et al. The Neuropeptide Cortistatin Alleviates Neuropathic Pain in Experimental Models of Peripheral Nerve Injury. Pharmaceutics. 2021;13:947.

12. Serrano-Martínez I, Pedreño M, Castillo-González J, Ferraz-de-Paula V, Vargas-Rodríguez P, Forte-Lago I, et al. Cortistatin as a Novel Multimodal Therapy for the Treatment of Parkinson's Disease. Int J Mol Sci. 2024;25:694.

13. Castillo-González J, Ruiz JL, Serrano-Martínez I, Forte-Lago I, Ubago-Rodriguez A, Caro M, et al. Cortistatin deficiency reveals a dysfunctional brain endothelium with impaired gene pathways, exacerbated immune activation, and disrupted barrier integrity. J Neuroinflammation. 2023;20:226.

14. Buscemi L, Price M, Bezzi P, Hirt L. Spatio-temporal overview of neuroinflammation in an experimental mouse stroke model. Sci Rep. 2019;9:507.

15. Buscemi L, Price M, Castillo-González J, Chatton J-Y, Hirt L. Lactate Neuroprotection against Transient Ischemic Brain Injury in Mice Appears Independent of HCAR1 Activation. Metabolites. 2022;12:465.

16. Lee S, Hong Y, Park S, Lee S-R, Chang K-T, Hong Y. Comparison of surgical methods of transient middle cerebral artery occlusion between rats and mice. J Vet Med Sci. 2014;76:1555–61.

17. Fernández-Arjona M del M, Grondona JM, Granados-Durán P, Fernández-Llebrez P, López-Ávalos MD. Microglia Morphological Categorization in a Rat Model of Neuroinflammation by Hierarchical Cluster and Principal Components Analysis. Front Cell Neurosci. 2017;11:235.

18. Young K, Morrison H. Quantifying Microglia Morphology from Photomicrographs of Immunohistochemistry Prepared Tissue Using ImageJ. JoVE. 2018;57648.

19. Schindelin J, Arganda-Carreras I, Frise E, Kaynig V, Longair M, Pietzsch T, et al. Fiji: an open-source platform for biological-image analysis. Nat Methods. 2012;9:676–82.

20. Türeyen K, Vemuganti R, Sailor KA, Dempsey RJ. Infarct volume quantification in mouse focal cerebral ischemia: a comparison of triphenyltetrazolium chloride and cresyl violet staining techniques. J Neurosci Methods. 2004;139:203–7.

21. Peng L, Hu G, Yao Q, Wu J, He Z, Law BY-K, et al. Microglia autophagy in ischemic stroke: A double-edged sword. Front Immunol. 2022;13.

22. Karperien A, Ahammer H, Jelinek H. Quantitating the subtleties of microglial morphology with fractal analysis. Front Cell Neurosci. 2013;7:3.

23. Linnerbauer M, Rothhammer V. Protective Functions of Reactive Astrocytes Following Central Nervous System Insult. Front Immunol. 2020;11:755955.

24. Thal S, Luh C, Schaible E-V, Timaru-Kast R, Hedrich J, Luhmann H, et al. Volatile Anesthetics Influence Blood-Brain Barrier Integrity by Modulation of Tight Junction Protein Expression in Traumatic Brain Injury. PloS one. 2012;7:e50752.

25. Abdullahi W, Tripathi D, Ronaldson PT. Blood-brain barrier dysfunction in ischemic stroke: targeting tight junctions and transporters for vascular protection. Am J Physiol Cell Physiol. 2018;315:C343–56.

26. Jiao H, Wang Z, Liu Y, Wang P, Xue Y. Specific Role of Tight Junction Proteins Claudin-5, Occludin, and ZO-1 of the Blood–Brain Barrier in a Focal Cerebral Ischemic Insult. J Mol Neurosci. 2011;44:130–9.

27. Rust R. Insights into the dual role of angiogenesis following stroke. J Cereb Blood Flow Metab. 2020;40:1167–71.

28. Iadecola C, Anrather J. The immunology of stroke: from mechanisms to translation. Nat Med. 2011;17:796–808.

29. Iadecola C, Buckwalter MS, Anrather J. Immune responses to stroke: mechanisms, modulation, and therapeutic potential. J Clin Invest. 2020;130:2777–88.

30. Barriga M, Benitez R, Robledo G, Caro M, O'Valle F, Campos-Salinas J, et al. Neuropeptide Cortistatin Regulates Dermal and Pulmonary Fibrosis in an Experimental Model of Systemic Sclerosis. Neuroendocrinology. 2021;112:784–95.

31. Benitez R, Forte-Lago I, Morell M, Maganto-Garcia E, Souza-Moreira L, O'Valle F, et al. Cortistatin reduces atherosclerosis in hyperlipidemic ApoE-deficient mice and the formation of foam cells. Sci Rep. 2017;7:46444.

32. Duran-Prado M, Morell M, Delgado-Maroto V, Castaño JP, Aneiros-Fernandez J, de Lecea L, et al. Cortistatin Inhibits Migration and Proliferation of Human Vascular Smooth Muscle Cells and Decreases Neointimal Formation on Carotid Artery Ligation. Circ Res. 2013;112:1444–55.

33. Benitez R, Caro M, Andres-Leon E, O'Valle F, Delgado M. Cortistatin regulates fibrosis and myofibroblast activation in experimental hepatotoxic- and cholestatic-induced liver injury. Br J Pharmacol. 2022;179:2275–96.

34. Yousufuddin M, Young N. Aging and ischemic stroke. Aging (Albany NY). 2019;11:2542–4.

35. Ritzel RM, Lai Y-J, Crapser JD, Patel AR, Schrecengost A, Grenier JM, et al. Aging alters the immunological response to ischemic stroke. Acta Neuropathol. 2018;136:89–110.

36. Sieber MW, Claus RA, Witte OW, Frahm C. Attenuated Inflammatory Response in Aged Mice Brains following Stroke. PLoS One. 2011;6:e26288.

37. Morell M, Souza-Moreira L, Caro M, O'Valle F, Forte-Lago I, de Lecea L, et al. Analgesic effect of the neuropeptide cortistatin in murine models of arthritic inflammatory pain. Arthritis Rheum. 2013;65:1390–401.

38. Bieber M, Gronewold J, Scharf A-C, Schuhmann MK, Langhauser F, Hopp S, et al. Validity and Reliability of Neurological Scores in Mice Exposed to Middle Cerebral Artery Occlusion. Stroke. 2019;50:2875–82.

39. Fan C, Zhang L, He Z, Shao P, Ding L, Wang G, et al. Reduced Severity of Outcome of Recurrent Ipsilateral Transient Cerebral Ischemia Compared with Contralateral Transient Cerebral Ischemia in Rats. J Stroke Cerebrovasc Dis. 2017;26:2915–25.

40. Barriga M, Benitez R, Ferraz-de-Paula V, Garcia-Frutos M, Caro M, Robledo G, et al. Protective role of cortistatin in pulmonary inflammation and fibrosis. Br J Pharmacol. 2021;178:4368–88.

41. Fluri F, Schuhmann MK, Kleinschnitz C. Animal models of ischemic stroke and their application in clinical research. Drug Des Devel Ther. 2015;9:3445–54.

42. Kharlamov A, LaVerde GC, Nemoto EM, Jungreis CA, Yushmanov VE, Jones SC, et al. MAP2 immunostaining in thick sections for early ischemic stroke infarct volume in non-human primate brain. J Neurosci Methods. 2009;182:205–10.

43. Pinto R, Magalhães A, Sousa M, Melo L, Lobo A, Barros P, et al. Bridging the Transient Intraluminal Stroke Preclinical Model to Clinical Practice: From Improved Surgical Procedures to a Workflow of Functional Tests. Front Neurol. 2022;13:846735.

44. Popa-Wagner A, Carmichael ST, Kokaia Z, Kessler C, Walker L. The Response of the Aged Brain to Stroke: Too Much, Too Soon? Curr Neurovasc Res. 2007;4:216–27.

45. Gullotta GS, De Feo D, Friebel E, Semerano A, Scotti GM, Bergamaschi A, et al. Age-induced alterations of granulopoiesis generate atypical neutrophils that aggravate stroke pathology. Nat Immunol. 2023;24:925–40.

46. Rubio A, Sánchez-Mut JV, García E, Velasquez ZD, Oliver J, Esteller M, et al. Epigenetic control of somatostatin and cortistatin expression by β amyloid peptide. J Neurosci Res. 2012;90:13–20.

47. Jia J, Yang L, Chen Y, Zheng L, Chen Y, Xu Y, et al. The Role of Microglial Phagocytosis in Ischemic Stroke. Front Immunol. 2022;12:790201.

48. Kawabori M, Kacimi R, Kauppinen T, Calosing C, Kim JY, Hsieh CL, et al. Triggering Receptor Expressed on Myeloid Cells 2 (TREM2) Deficiency Attenuates Phagocytic Activities of Microglia and Exacerbates Ischemic Damage in Experimental Stroke. J Neurosci. 2015;35:3384–96.

49. Neher JJ, Emmrich JV, Fricker M, Mander PK, Théry C, Brown GC. Phagocytosis executes delayed neuronal death after focal brain ischemia. Proc Natl Acad Sci U S A. 2013;110:E4098–107.

50. Pérez Falo C. Papel del neuropéptido cortistatina en la fisiopatología de los procesos de des- y remielinización en el sistema nervioso. Doctoral Thesis University of Granada; 2021.

51. Jolivel V, Bicker F, Binamé F, Ploen R, Keller S, Gollan R, et al. Perivascular microglia promote blood vessel disintegration in the ischemic penumbra. Acta Neuropathol. 2015;129:279–95.

52. Xu X, Gao W, Li L, Hao J, Yang B, Wang T, et al. Annexin A1 protects against cerebral ischemia–reperfusion injury by modulating microglia/macrophage polarization via FPR2/ALX-dependent AMPK-mTOR pathway. J Neuroinflammation. 2021;18:119.

53. Paolicelli RC, Sierra A, Stevens B, Tremblay M-E, Aguzzi A, Ajami B, et al. Microglia states and nomenclature: A field at its crossroads. Neuron. 2022;110:3458–83.

54. Fan P, Wang S, Chu S, Chen N. Time-dependent dual effect of microglia in ischemic stroke. Neurochem Int. 2023;169:105584.

55. Wen Q, Ding Q, Wang J, Yin Y, Xu S, Ju Y, et al. Cortistatin-14 Exerts Neuroprotective Effect Against Microglial Activation, Blood-brain Barrier Disruption, and Cognitive Impairment in Sepsis-associated Encephalopathy. J Immunol Res. 2022;2022:3334145.

56. Fujikawa R, Jinno S. Identification of hyper-ramified microglia in the CA1 region of the mouse hippocampus potentially associated with stress resilience. Eur J Neurosci. 2022;56:5137–53.

57. Vidal-Itriago A, Radford RAW, Aramideh JA, Maurel C, Scherer NM, Don EK, et al. Microglia morphophysiological diversity and its implications for the CNS. Front Immunol. 2022;13:997786.

58. Li F, Zhao H, Han Z, Wang R, Tao Z, Fan Z, et al. Xuesaitong May Protect Against Ischemic Stroke by Modulating Microglial Phenotypes and Inhibiting Neuronal Cell Apoptosis via the STAT3 Signaling Pathway. CNS Neurol Disord Drug Targets. 2019;18:115–23.

59. Wang D, Liu F, Zhu L, Lin P, Han F, Wang X, et al. FGF21 alleviates neuroinflammation following ischemic stroke by modulating the temporal and spatial dynamics of microglia/macrophages. J Neuroinflammation. 2020;17:257.

60. Shen X-Y, Gao Z-K, Han Y, Yuan M, Guo Y-S, Bi X. Activation and Role of Astrocytes in Ischemic Stroke. Front Cell Neurosci. 2021;15:755955.

61. Burda JE, Sofroniew MV. Reactive Gliosis and the Multicellular Response to CNS Damage and Disease. Neuron. 2014;81:229–48.

62. Wanner IB, Anderson MA, Song B, Levine J, Fernandez A, Gray-Thompson Z, et al. Glial Scar Borders Are Formed by Newly Proliferated, Elongated Astrocytes That Interact to Corral Inflammatory and Fibrotic Cells via STAT3-Dependent Mechanisms after Spinal Cord Injury. J Neurosci. 2013;33:12870–86.

63. Li L, Zhou J, Han L, Wu X, Shi Y, Cui W, et al. The Specific Role of Reactive Astrocytes in Stroke. Front Cell Neurosci. 2022;16:850866.

64. Faulkner JR, Herrmann JE, Woo MJ, Tansey KE, Doan NB, Sofroniew MV. Reactive astrocytes protect tissue and preserve function after spinal cord injury. J Neurosci. 2004;24:2143–55.

65. Candelario-Jalil E, Dijkhuizen RM, Magnus T. Neuroinflammation, Stroke, Blood-Brain Barrier Dysfunction, and Imaging Modalities. Stroke. 2022;53:1473–86.

66. Bernardo-Castro S, Sousa JA, Brás A, Cecília C, Rodrigues B, Almendra L, et al. Pathophysiology of Blood–Brain Barrier Permeability Throughout the Different Stages of Ischemic Stroke and Its Implication on Hemorrhagic Transformation and Recovery. Front Neurol. 2020;11: :594672.

67. Gonzalez-Rey E, Chorny A, Robledo G, Delgado M. Cortistatin, a new antiinflammatory peptide with therapeutic effect on lethal endotoxemia. J Exp Med. 2006;203:563–71.

68. Famakin BM. The Immune Response to Acute Focal Cerebral Ischemia and Associated Post-stroke Immunodepression: A Focused Review. Aging Dis. 2014;5:307–26.

69. Doll DN, Barr TL, Simpkins JW. Cytokines: Their Role in Stroke and Potential Use as Biomarkers and Therapeutic Targets. Aging Dis. 2014;5:294–306.

70. Pawluk H, Woźniak A, Grześk G, Kołodziejska R, Kozakiewicz M, Kopkowska E, et al. The Role of Selected Pro-Inflammatory Cytokines in Pathogenesis of Ischemic Stroke. Clin Interv Aging. 2020;15:469–84..

71. Bustamante A, Sobrino T, Giralt D, García-Berrocoso T, Llombart V, Ugarriza I, et al. Prognostic value of blood interleukin-6 in the prediction of functional outcome after stroke: A systematic review and meta-analysis. J Neuroimmunol. 2014;274:215–24.

72. Shaafi S, Sharifipour E, Rahmanifar R, Hejazi S, Andalib S, Nikanfar M, et al. Interleukin-6, a reliable prognostic factor for ischemic stroke. Iran J Neurol. 2014;13:70–6.

73. Fang W, Zhai X, Han D, Xiong X, Wang T, Zeng X, et al. CCR2-dependent monocytes/macrophages exacerbate acute brain injury but promote functional recovery after ischemic stroke in mice. Theranostics. 2018;8:3530–43.

74. Qin C, Yang S, Chu Y-H, Zhang H, Pang X-W, Chen L, et al. Signaling pathways involved in ischemic stroke: molecular mechanisms and therapeutic interventions. Sig Transduct Target Ther. 2022;7:1–29.

75. Gertz K, Kronenberg G, Kälin RE, Baldinger T, Werner C, Balkaya M, et al. Essential role of interleukin-6 in post-stroke angiogenesis. Brain. 2012;135:1964–80.

76. Grønhøj MH, Clausen BH, Fenger CD, Lambertsen KL, Finsen B. Beneficial potential of intravenously administered IL-6 in improving outcome after murine experimental stroke. Brain, Behav Immun. 2017;65:296–311.

77. Cao Y, Yue X, Jia M, Wang J. Neuroinflammation and anti-inflammatory therapy for ischemic stroke. Heliyon. 2023;9:e17986.

78. Rauca C, Schäfer K, Höllt V. Effects of somatostatin, octreotide and cortistatin on ischaemic neuronal damage following permanent middle cerebral artery occlusion in the rat. Naunyn-Schmiedeberg's Arch Pharmacol. 1999;360:633–8.

79. Cheyuo C, Wu R, Zhou M, Jacob A, Coppa G, Wang P. Ghrelin Suppresses Inflammation and Neuronal Nitric Oxide Synthase in Focal Cerebral Ischemia Via the Vagus Nerve. Shock. 2011;35:258.

80. Miao Y, Xia Q, Hou Z, Zheng Y, Pan H, Zhu S. Ghrelin protects cortical neuron against focal ischemia/reperfusion in rats. Biochem Biophys Res Commun. 2007;359:795–800.

81. Seyhanli ES, Lok U, Gulacti U, Buyukaslan H, Atescelik M, Yildiz M, et al. Assessment of serum and urine ghrelin levels in patients with acute stroke. Int J Clin Exp Med. 2015;8:722–9.

82. Xu X, Zhu Y, Chuai J. Changes in Serum Ghrelin and Small Intestinal Motility in Rats with Ischemic Stroke. Anat Rec (Hoboken). 2012;295:307–12.

83. Delgado-Maroto V, Benitez R, Forte-Lago I, Morell M, Maganto-Garcia E, Souza-Moreira L, et al. Cortistatin reduces atherosclerosis in hyperlipidemic ApoE-deficient mice and the formation of foam cells. Sci Rep. 2017;7:46444.

84. Stumm RK. Somatostatin Receptor 2 Is Activated in Cortical Neurons and Contributes to Neurodegeneration after Focal Ischemia. J Neurosci. 2004;24:11404–15.

85. Gahete MD, Rubio A, Durán-Prado M, Avila J, Luque RM, Castaño JP. Expression of Somatostatin, cortistatin, and their receptors, as well as dopamine receptors, but not of neprilysin, are reduced in the temporal lobe of Alzheimer's disease patients. J Alzheimers Dis. 2010;20:465–75.

86. Carrasco E, Hernández C, de Torres I, Farrés J, Simó R. Lowered cortistatin expression is an early event in the human diabetic retina and is associated with apoptosis and glial activation. Mol Vis. 2008;14:1496–502.

87. Souza-Moreira L, Campos-Salinas J, Caro M, Gonzalez-Rey E. Neuropeptides as Pleiotropic Modulators of the Immune Response. Neuroendocrinology. 2011;94:89–100.